

Aspects of Quasi-Phasestructure of the Schwinger Model on a Cylinder with Broken Chiral Symmetry

Stephan Dürr

University of Washington
Particle Theory Group, Box 351560
Seattle, WA 98195 (U.S.A.)
durr@phys.washington.edu

Abstract

We consider the N_f -flavour Schwinger Model on a thermal cylinder of circumference $\beta = 1/T$ and of finite spatial length L . On the boundaries $x^1 = 0$ and $x^1 = L$ the fields are subject to an element of a one-dimensional class of bag-inspired boundary conditions which depend on a real parameter θ and break the axial flavour symmetry. For the cases $N_f = 1$ and $N_f = 2$ all integrals can be performed analytically. While general theorems do not allow for a nonzero critical temperature, the model is found to exhibit a quasi-phase-structure: For finite L the condensate – seen as a function of $\log(T)$ – stays almost constant up to a certain temperature (which depends on L), where it shows a sharp crossover to a value which is exponentially close to zero. In the limit $L \rightarrow \infty$ the known behaviour for the one-flavour Schwinger model is reproduced. In case of two flavours direct pictorial evidence is given that the theory undergoes a phase-transition at $T_c = 0$. The latter is confirmed – as predicted by Smilga and Verbaarschot – to be of second order but for the critical exponent δ the numerical value is found to be 2 which is at variance with their bosonization-rule based prediction $\delta = 3$.

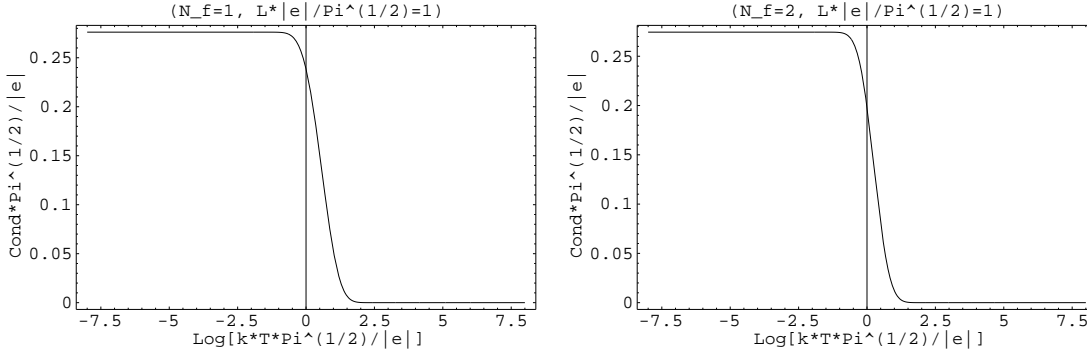


Figure 1: The (dimensionless) condensate $|\langle\psi^\dagger P_\pm\psi\rangle|/\mu_1$ as a function of $\log(kT/\mu_1)$ at fixed box-length $L = 1/\mu_1$ (where $\mu_1 = |e|/\pi^{1/2}$ is the induced single-flavour Schwinger mass (5)) for $N_f = 1$ and $N_f = 2$.

1 Introduction

For realistic gauge field theories like QCD(4) it is in general an unsolved problem to determine their phase-structure (e.g. as a function of the fermion masses $m_1 \dots m_{N_f}$) analytically. For this reason, one may either determine their phase-structure approximatively or try to attack the question in some simpler models analytically [1, 2].

For many questions arising in QCD, the Schwinger model [3] (QED in two dimensions with one or N_f massless fermions) has proven to be an interesting testing ground: It has shed some light on such longstanding problems of QCD as the $U(1)_A$ -problem [4] and it has been used to test the validity of the Instanton Liquid Picture [5, 6].

However, for investigating symmetry-breakdown any two-dimensional model field theory doesn't seem to be of interest: There is no spontaneous breaking of a continuous global symmetry with associated Goldstone bosons in two dimensions [7] and a symmetry which is anomalously broken can't get restored at finite temperature [8].

It is the aim of the present paper to show that – in spite of the truth of this conventional wisdom – the Schwinger model exhibits an interesting quasi-phase-structure: The chiral condensate $\langle\psi^\dagger \frac{1}{2}(1 \pm \gamma_5)\psi\rangle$ (which is used to probe the chiral symmetry) shows – as a function of the log of the temperature – a sharp crossover-behaviour: For any finite box-length L there is a well defined low-temperature regime where the condensate stays almost constant (the value depends on L) and there is a “critical temperature” where the condensate decays (through a fairly well localized symmetry-quasi-restoration process) to a value which is exponentially close (but not equal) to zero.

Moreover, as the length L is sent to infinity, this behaviour is shown to provide direct evidence that the two-flavour Schwinger model exhibits a phase-transition at $T_c=0$ and that the latter is of second order – which is an assumption-free rederivation of a recent claim by Smilga and Verbaarschot [9].

The Schwinger model has had a great impact on the development of field-theoretic ideas and techniques: The original quantization on the plane [10] suffered from the deficit that a direct calculation of the condensates $\langle\psi^\dagger\psi\rangle$ and $\langle\psi^\dagger\gamma_5\psi\rangle$ gave vanishing results whereas an indirect determination via the clustering theorem led to the standard nonzero value [11]. One decade ago the Schwinger model has been quantized on compact manifolds without boundaries, the first ones being the (euclidean) sphere S^2 [12] and the (euclidean) torus T^2

[13]. In either case direct calculations for the chiral condensates $\langle\psi^\dagger\psi\rangle$ and $\langle\psi^\dagger\gamma_5\psi\rangle$ were found to yield nonvanishing results for a finite volume of the manifold.

Here we shall consider the model on a finite-temperature-cylinder with (anti-)periodic boundary conditions in the euclidean timelike direction, but with noncyclic boundary conditions in the spatial direction: On the two spatial ends (at $x^1=0$ and $x^1=L$) some chirality-breaking (XB-) boundary-conditions are imposed.

The motivation to use these XB-boundary-conditions stems again from QCD. There one would like to give a proof (without involving any assumption) that in the chiral limit the axial flavour symmetry $SU(N_f)_A$ is spontaneously broken. The natural way to study a symmetry which is expected to be broken spontaneously is to break it explicitly and to try to determine how the system behaves in the limit when the external trigger is softly removed. For both QCD and the N_f -flavour Schwinger model this means that one has to break the axial N_f -flavour symmetry and then try to determine how some observables which are sensitive to its breaking do behave in the limit where the trigger term is removed. There is a long series of efforts in the literature which try to achieve this goal by studying either QCD or the N_f -flavour Schwinger model with a small fermion mass. In this approach the task is to determine how the chiral correlators behave in the limit where the fermion masses tend to be tiny as compared to the intrinsic mass of the theory. The problem with this particular method of breaking the axial flavour symmetry is that the value of the chiral condensate is related to the mean level density of the eigenvalues of the Dirac operator in the infrared [14], but the spectral density of the massive Dirac operator in a given gauge-field background is not (yet) known in general.

Together with A.Wipf, we have previously explored the alternative of breaking the chiral symmetry through introducing boundary conditions for the fermions rather than giving them a mass [15]. There we dealt with euclidean $U(N_c)$ and $SU(N_c)$ gauge-theories with N_f massless flavours quantized inside an even($d=2n$)-dimensional ball B_R^{2n} with boundary S_R^{2n-1} on which the XB-boundary-conditions considered in [16] have been imposed. These boundary conditions relate the different spin-components of each flavour on the boundary and are neutral with respect to vector-flavour-transformations. As a consequence the (gauge-invariant) fermionic determinant is the same for all flavours. The most important result of this work was the observation that the XB-boundary-conditions proved to be equally suited to trigger a chiral condensate as small fermion masses are. From a technical point of view, the XB-boundary-conditions turned out to be very convenient: In abelian theories, the (massless) fermionic determinant can be calculated in an arbitrary gauge-field background (the fields subject to the XB-boundary-conditions) and thus we derived in two dimensions the analytical expressions for the chiral correlators (exploiting the rotational symmetry of B^2).

In a second work [17], we examined whether the approach of breaking the $SU(N_f)_A$ -symmetry by boundary-conditions can be extended to gauge-systems at finite temperature. Choosing the Schwinger model as a testbed the answer was in the affirmative: First of all we found that most of the nice features associated to the quantization on contractible manifolds (topologically equivalent to B^{2n}) persist in the case of the finite temperature cylinder with XB-boundary-conditions at the spatial ends: The configuration space is still *topologically trivial* (i.e. without disconnected instanton sectors) and in particular there are *no fermionic zero-modes* (which usually tend to complicate the quantization considerably [13]). The technical difficulty we had to deal with is the fact that on non-contractible manifolds (e.g. a cylinder) the standard decomposition-technique for the Dirac operator, on which the quantization adopted in [15] heavily relied, could no longer be used. For this reason [17] turned out

to be a rather technical paper, mostly devoted to show how this difficulty can be overcome.

The present paper concentrates on the physics which can be addressed from this setup. To be definite: The Schwinger model

$$S[A, \psi^\dagger, \psi] = S_B[A] + S_F[A, \psi^\dagger, \psi] \quad (1)$$

$$S_B = \frac{1}{4} \int_M F_{\mu\nu} F_{\mu\nu} \quad , \quad S_F = \sum_{n=1}^{N_f} \int_M \psi_n^\dagger i \not{D} \psi_n$$

in $d = 2$ dimensions is studied on the manifold

$$M = [0, \beta] \times [0, L] \quad \ni \quad (x^0, x^1) \quad (2)$$

with volume $V = \beta L$. In euclidean time direction, the fields A and ψ are periodic and antiperiodic respectively with period β . Hence $x^0 = 0$ and $x^0 = \beta$ are identified (up to an eventual minus sign) and the manifold is a cylinder. At the spatial ends of the cylinder (at $x^1 = 0$ and $x^1 = L$) specific XB-boundary-conditions (to be discussed below) are imposed. Through explicit numerical evaluation of the analytical formulae we demonstrate that the model exhibits a quasi-phase-structure as described above. In particular we find that the two-flavour Schwinger model (limit $L \rightarrow \infty$) exhibits a (true) phase-transition at $T_c = 0$ and that the latter is of second order – which is a rederivation of a result which was obtained by Smilga and Verbaarschot [9] using completely different technical tools.

For notational simplicity we use the abbreviations

$$\tau = \frac{\beta}{2L} \quad , \quad \xi = \frac{x^1}{L} \quad (3)$$

as well as the dimensionless inverse temperature and box-length

$$\sigma \equiv \frac{|e|\beta}{\sqrt{\pi}} \quad , \quad \lambda \equiv \frac{|e|L}{\sqrt{\pi}} \quad (4)$$

which are built from β, L by rescaling them with the Compton-wavelength associated to the single-flavour Schwinger-mass μ_1 where

$$\mu : \equiv \sqrt{\frac{N_f e^2}{\pi}} \quad (5)$$

is the generalization of μ_1 to the case of N_f -flavours.

This paper is organized as follows: In section 2 we briefly review the quantization of the model subject to the XB-boundary-conditions. In section 3 the analytical results for the chiral condensate $\langle \psi^\dagger \frac{1}{2}(1 \pm \gamma_5) \psi \rangle(x)$ are re-expressed using theta-functions. In section 4 the remaining (c-number-)integrals within the analytic formulae for arbitrary N_f are fully performed for the cases $N_f = 1$ and $N_f = 2$. This allows us to show explicit numerical evaluations of our analytical findings for these two cases revealing the two quasi-phases as described above and resulting in an explicit plot of the “quasi-phase-structure” figure 7. In the concluding section 5 we try to illustrate our results and to relate them to the work by Smilga and Verbaarschot [9] and others.

2 Quantization with Thermal and XB-Boundary-Conditions

Here we shall give a short review of the conceptually relevant aspects of the quantization. For technical aspects the reader is referred to [17].

2.1 Chirality Breaking Boundary Conditions

The chirality-breaking (XB-)boundary-conditions as discussed in [16] can be motivated by the request that the Dirac operator $i\mathcal{D}$ is symmetric under the scalar product $(\chi, \psi) := \int \chi^\dagger \psi d^2x$, which leads to the condition that the surface integral $i \oint \chi^\dagger \gamma_n \psi ds$ vanishes, where $\gamma_n = (\gamma, n) = n_\mu \gamma_\mu = \not{n}$ and n_μ is the outward oriented normal vectorfield on the boundary. Imposing local linear boundary conditions which ensure this requirement amounts to have $\chi^\dagger \gamma_n \psi = 0$ on the boundary for each pair. A sufficient condition is to have all modes obeying $\psi = B\psi$ on the boundary, where the boundary operator B (which is understood to act as the identity in flavour space) is required to satisfy $B^\dagger \gamma_n B = -\gamma_n$ and $B^2 = 1$. We shall choose the one-parameter family of boundary operators [16]

$$B \equiv B_\theta := i\gamma_5 e^{\theta\gamma_5} \gamma_n \quad (6)$$

which break the γ_5 -invariance of the theory, thus making the N_f flavour theory invariant under $SU(N_f)_V$ instead of $SU(N_f)_L \times SU(N_f)_R$. They will be supplemented by suitable boundary conditions for the gauge-field. These boundary conditions prevent the $U(1)$ -current from leaking through the boundary as they ensure $j \cdot n = \psi^\dagger \gamma_n \psi = 0$ on the boundary.

For explicit calculations we shall choose the chiral representation $\gamma_0 = \sigma_1, \gamma_1 = \sigma_2$ and $\gamma_5 = \sigma_3$ which implies that the explicit expressions for the boundary operators at the two ends of the cylinder (2) take the simple form

$$B_L = - \begin{pmatrix} 0 & e^\theta \\ e^{-\theta} & 0 \end{pmatrix} \text{ (at } x^1=0) \quad \text{and} \quad B_R = + \begin{pmatrix} 0 & e^\theta \\ e^{-\theta} & 0 \end{pmatrix} \text{ (at } x^1=L) \quad . \quad (7)$$

2.2 Immediate Consequences for the Spectrum

The decision to quantize with boundary condition $\psi = B_\theta \psi$ with the boundary operator (6) has immediate consequences [15, 17, 18]:

- (i) The Dirac operator has a discrete real spectrum which is *asymmetric* w.r.t. zero.
- (ii) The spectrum is empty at zero, i.e. the Dirac operator has *no zero modes*.
- (iii) The instanton number $q = \frac{e}{4\pi} \int \epsilon_{\mu\nu} F_{\mu\nu} = \frac{e}{2\pi} \int E \in \mathbf{R}$ is *not quantized*.

The first property already indicates that we are not in the situation covered by the Atiyah-Patodi-Singer-index-theorem. The second property implies that the generating functional for the fermions in a given gauge-field background A

$$Z_F[A, \eta^\dagger, \eta] = \frac{1}{N_F} \int D\psi^\dagger D\psi e^{-\int \psi^\dagger i\mathcal{D}\psi + i \int \psi^\dagger \eta - i \int \eta^\dagger \psi} \quad (8)$$

is indeed given by the textbook formula

$$Z_F[A, \eta^\dagger, \eta] = \frac{\det_\theta(i\mathcal{D})}{\det_\theta(i\mathcal{D})} e^{\int \eta^\dagger (i\mathcal{D})^{-1} \eta} \quad (9)$$

and the chiral expectation values follow by taking the logarithmic derivative

$$\langle \psi^\dagger(x) P_\pm \psi(x) \rangle = \frac{1}{Z_F} \frac{\delta^2}{\delta \eta_\pm(x) \delta \eta_\pm^\dagger(x)} Z_F \Big|_{\eta_\pm = \eta_\pm^\dagger = 0} . \quad (10)$$

Throughout θ is the free parameter in the boundary operator (7). The fact that the Feynman-Hellmann-boundary-formula $\frac{d}{d\theta} \lambda_k = -\lambda_k(\psi_k, \gamma_5 \psi_k)$ [19] (where the λ_k denote the eigenvalues of $i\mathcal{D}$) still holds true on the cylinder was the basis for the analytic determination of the θ -dependence of the fermionic determinant $\det_\theta(i\mathcal{D})$ performed in [17].

2.3 Neither Integer nor Fractional but Real Instanton Number

On a cylinder of finite spatial length the decomposition of a gauge potential A_μ is [17]

$$\begin{aligned} eA_0 &= -\partial_1 \phi + \partial_0 \chi + \frac{2\pi}{\beta} c \\ eA_1 &= +\partial_0 \phi + \partial_1 \chi \end{aligned} \quad (11)$$

where ϕ obeys Dirichlet boundary conditions at the ends ($x^1 = 0, L$) and χ is a pure gauge degree of freedom which fulfills $\chi(0) + \chi(L) = 0$ and $c \in [-1/2, 1/2[$ is the constant harmonic part. Thus the Dirac operator $i\mathcal{D} = i\gamma_\mu(\partial_\mu - ieA_\mu)$ may be factorized

$$i\mathcal{D} = G^\dagger i\mathcal{D}_0 G \quad (12)$$

where $i\mathcal{D}_0 = \gamma^0(i\partial_0 + 2\pi c/\beta) + \gamma^1 i\partial_1$ is the Dirac operator with the scalar parts switched off and $G = \text{diag}(g^{*-1}, g)$ contains the prepotential $g := e^{-(\phi+i\chi)}$ which is an element of the complexified gauge-group $U(1)^* = S^1 \times \mathbf{R}_+$.

On the cylinder there is a one-to-one-correspondence between ϕ and eF_{01} if ϕ obeys Dirichlet boundary-conditions at the two ends. The general field ϕ may be decomposed as

$$\phi = \sum_{m \geq 0} \sum_{n \geq 1} \phi_{mn}^+ \cos\left(\frac{2\pi m x^0}{\beta}\right) \sin\left(\frac{\pi n x^1}{L}\right) + \phi_{mn}^- \sin\left(\frac{2\pi m x^0}{\beta}\right) \sin\left(\frac{\pi n x^1}{L}\right) \quad (13)$$

with coefficients $\phi_{mn}^\pm \in \mathbf{R}$ decaying rapidly enough to make the series converge. The instanton-number is given by

$$q = \frac{e}{2\pi} \int E \, d^2x = \frac{1}{2\pi} \int \Delta \phi \, d^2x = -\frac{\beta}{L} \sum_{n \geq 1} \frac{1 - (-1)^n}{2} n \phi_{0n}^+ \quad (14)$$

where the decomposition (11) and the expansion (13) have been used. Given the result (14) it is obvious that the instanton-number q may take any real number.

2.4 Fermionic Propagator w.r.t. Boundary Conditions

In order to calculate the condensates one needs the Green's function S_θ of the Dirac operator $i\mathcal{D}$ on the cylinder subject to the XB-boundary-conditions. In addition to the defining relation $(i\mathcal{D} S_\theta)(x, y) = \delta(x - y)$ this Green's function obeys the boundary-conditions

$$S_\theta(x^0 + \beta, x^1, y) = -S_\theta(x, y) \quad (15)$$

$$(B_L S_\theta)(x^0, x^1 = 0, y) = S_\theta(x^0, x^1 = 0, y) \quad (16)$$

$$(B_R S_\theta)(x^0, x^1 = L, y) = S_\theta(x^0, x^1 = L, y) \quad (17)$$

with $B_{L/R}$ defined in (7) plus the adjoint relations with respect to y . The dependence of the gauge-potential has not been made explicit, since from the factorization-property (12) for the Dirac-operator it follows at once that S_θ is related to the Green's function \tilde{S}_θ of $i\mathcal{D}_0$ as

$$S_\theta(x, y) = G^{-1}(x)\tilde{S}_\theta(x, y)G^{\dagger -1}(y) . \quad (18)$$

Since the field ϕ obeys Dirichlet boundary-conditions at the ends of the cylinder, the deformation matrix G appearing in (12) is unitary there and the boundary-conditions (15-17) transform into the identical ones for

$$\tilde{S}_\theta(x, y) = \begin{pmatrix} \tilde{S}_{++} & \tilde{S}_{+-} \\ \tilde{S}_{-+} & \tilde{S}_{--} \end{pmatrix}$$

where the indices refer to chirality. This Green's function – which carries the full c -dependence of $S_\theta(x, y)$ – has been determined analytically [17] to read

$$\tilde{S}_\theta(x, y) = \frac{i}{2\pi} \cdot \sum_{m, n \in \mathbb{Z} \times \mathbb{Z}} (-1)^{(m+n)} \cdot e^{2\pi ic((x^0-y^0)/\beta-n)} \cdot \begin{pmatrix} e^\theta/r_{nm} & -(1/s_{nm}) \\ -(1/\bar{s}_{nm}) & e^{-\theta}/\bar{r}_{nm} \end{pmatrix}, \quad (19)$$

where $r_{nm} = (x^0-y^0) + i(x^1+y^1) - (n\beta + 2imL)$ and $s_{nm} = (x^0-y^0) + i(x^1-y^1) - (n\beta + 2imL)$. From (19) it follows that the $++$ and $--$ elements at coinciding points inside the cylinder take the forms

$$\begin{aligned} \tilde{S}_\theta(x, x)_{\pm\pm} &= \pm \frac{e^{\pm\theta}}{4L} \sum_{n \in \mathbb{Z}} (-1)^n \frac{e^{\pm 2\pi inc}}{\sin(\pi(\xi - in\tau))} \\ &= \pm \frac{e^{\pm\theta}}{4L} \sum_{n \in \mathbb{Z}} (-1)^n \frac{\cos(2\pi nc) \sin(\pi\xi) \text{ch}(\pi n\tau) - \sin(2\pi nc) \cos(\pi\xi) \text{sh}(\pi n\tau)}{\sin^2(\pi\xi) + \text{sh}^2(\pi n\tau)} \end{aligned} \quad (20)$$

$$\begin{aligned} \tilde{S}_\theta(x, x)_{\pm\pm} &= \pm \frac{e^{\pm\theta}}{2\beta} \sum_{m \in \mathbb{Z}} (-1)^m \frac{e^{-2\pi(m+\xi)c/\tau}}{\sinh(\pi(m+\xi)/\tau)} \\ &= \pm \frac{e^{\pm\theta}}{2\beta} \sum_{m \in \mathbb{Z}} (-1)^m \frac{\text{ch}(2\pi(m+\xi)c/\tau) - \text{sh}(2\pi(m+\xi)c/\tau)}{\text{sh}(\pi(m+\xi)/\tau)} \end{aligned} \quad (21)$$

both valid for $c \in [-\frac{1}{2}, \frac{1}{2}]$. The two forms (20, 21) are equivalent but enjoy good convergence properties in the two regimes $\beta \gg L$ and $\beta \ll L$ respectively. From (18) one sees that the chirality violating entries of the fermionic Green's function lie on the diagonal and take the form

$$S_\theta(x; x)_{\pm\pm} = e^{\mp 2\phi(x)} \tilde{S}_\theta(x; x)_{\pm\pm} \quad (22)$$

where $\tilde{S}_{\pm\pm}$ plugged in from (20, 21) depends only on the harmonic part c in the decomposition (11) of the gauge-potential.

2.5 Fermionic Determinant w.r.t. Boundary Conditions

The arduous step is the computation of the θ -dependence of the fermionic-determinant [17]. The Dirac-operator and the boundary-conditions are both flavour-neutral. Thus the determinant is the same for all flavours and it is sufficient to calculate it for one flavour. For

the explicit calculations we used the gauge-invariant ζ -function definition of the determinant [20, 21]

$$\log \det_{\theta}(i\mathcal{D}) := \frac{1}{2} \log \det_{\theta}(-\mathcal{D}^2) := -\frac{1}{2} \frac{d}{ds} \Big|_{s=0} \zeta_{\theta}(-\mathcal{D}^2, s) \quad (23)$$

and calculated the θ -dependence of the ζ -function by means of a boundary-Feynman-Hellmann-formula. Denoting $\{\mu_k | k \in \mathbf{N}\}$ the (positive) eigenvalues of $-\mathcal{D}^2$, the corresponding ζ -function is defined and rewritten as a Mellin-transform in the usual way

$$\zeta_{\theta}(s) := \zeta_{\theta}(-\mathcal{D}^2, s) := \sum_k \mu_k^{-s} = \frac{1}{\Gamma(s)} \int_0^{\infty} t^{s-1} \text{tr}_{\theta}(e^{-t(-\mathcal{D}^2)}) dt \quad (24)$$

for $\text{Re}(s) > d/2 = 1$ and its analytic continuation to $\text{Re}(s) \leq 1$.

The general task was to compute the normalized determinant

$$\frac{\det_{\theta}(i\mathcal{D})}{\det_0(i\mathcal{D})} \equiv \frac{\det_{\theta}(i\mathcal{D}_{1,c})}{\det_0(i\mathcal{D}_{0,0})} \quad (25)$$

where the first suffix on the r.h.s. indicates whether the scalar part is switched on and the c refers to the harmonic part in the decomposition (11). Together with θ we thus have three parameters to switch off and this leaves us with $3! = 6$ possible choices how to compute the functional determinant (25) in terms of three factors where each involves one switching only. We explicitly followed two of the six choices and found them to agree.

Our first choice was to calculate the functional determinant according to

$$\frac{\det_{\theta}(i\mathcal{D}_{1,c})}{\det_0(i\mathcal{D}_{0,0})} \equiv \frac{\det_{\theta}(i\mathcal{D}_{1,c})}{\det_0(i\mathcal{D}_{1,c})} \cdot \frac{\det_0(i\mathcal{D}_{1,c})}{\det_0(i\mathcal{D}_{0,c})} \cdot \frac{\det_0(i\mathcal{D}_{0,c})}{\det_0(i\mathcal{D}_{0,0})} \quad (26)$$

where we got for the first factor the explicit expression

$$\frac{\det_{\theta}(i\mathcal{D}_{1,c})}{\det_0(i\mathcal{D}_{1,c})} = \exp\left\{-\frac{\theta}{4\pi} \int e\epsilon_{\mu\nu} F_{\mu\nu}\right\} = \exp\left\{-\frac{\theta}{2\pi} \int \Delta\phi\right\}. \quad (27)$$

to be multiplied with the result

$$\frac{\det_0(i\mathcal{D}_{1,c})}{\det_0(i\mathcal{D}_{0,c})} = \exp\left\{\frac{1}{2\pi} \int \phi\Delta\phi\right\} \quad (28)$$

for the second factor. It is worth noting that with the first choice the term linear in θ in the effective action stems from a volume-term (i.e. $a_1(\cdot)$) in the Seeley-DeWitt-expansion.

Our second choice was to calculate the functional determinant according to

$$\frac{\det_{\theta}(i\mathcal{D}_{1,c})}{\det_0(i\mathcal{D}_{0,0})} \equiv \frac{\det_{\theta}(i\mathcal{D}_{1,c})}{\det_{\theta}(i\mathcal{D}_{0,c})} \cdot \frac{\det_{\theta}(i\mathcal{D}_{0,c})}{\det_0(i\mathcal{D}_{0,c})} \cdot \frac{\det_0(i\mathcal{D}_{0,c})}{\det_0(i\mathcal{D}_{0,0})} \quad (29)$$

where we found for the first factor the explicit expression

$$\frac{\det_{\theta}(i\mathcal{D}_{1,c})}{\det_{\theta}(i\mathcal{D}_{0,c})} = \exp\left\{\frac{1}{2\pi} \int \phi\Delta\phi - \frac{\theta}{2\pi} \int \Delta\phi\right\} \quad (30)$$

to be multiplied with the result

$$\frac{\det_{\theta}(i\mathcal{D}_{0,c})}{\det_0(i\mathcal{D}_{0,c})} = \exp\{0\} = 1 \quad (31)$$

for the second factor. It is worth noting that with the second choice the term linear in θ in the effective action stems from a boundary-term (i.e. $b_1(\cdot)$) in the Seeley-DeWitt-expansion.

In summary, the scattering of the fermions off the boundary generates a CP-odd term linear in θ in the effective action for the gauge-bosons which may be seen as a two-dimensional artificial analogue of the QCD- θ -term.

The remaining task (which is to calculate the common third factor in the factorizations (26) and (29) of the functional determinant) was addressed by rewriting its logarithm as

$$\log \frac{\det_0(i\mathcal{D}_{0,c})}{\det_0(i\mathcal{D}_{0,0})} = -\frac{1}{2} \int_0^c \frac{d}{ds} \Big|_{s=0} \frac{d}{d\tilde{c}} \zeta_0(-\mathcal{D}_{0,\tilde{c}}^2, s) d\tilde{c} \quad . \quad (32)$$

and constructing the s -derivative at $s = 0$ of the \tilde{c} -derivative of $\zeta_0(-\mathcal{D}_{0,\tilde{c}}^2, s)$ explicitly. For that aim we computed the heat-kernel of the operator

$$-\mathcal{D}_{0,\tilde{c}}^2 = -\left((\partial_0 - 2\pi i\tilde{c}/\beta)^2 + \partial_1^2\right) I_2$$

for $\theta = 0$ on the half-cylinder (see appendix of [17]) and from this expression we were able to derive

$$\Gamma(c) \equiv -\log \frac{\det_0(i\mathcal{D}_{0,c})}{\det_0(i\mathcal{D}_{0,0})} = \frac{V}{\pi} \sum' (-1)^{m+n} \frac{\cos(2\pi n c) - 1}{(n\beta)^2 + (2mL)^2} \quad (33)$$

as the result for the negative of the logarithm of the last factor of (26) and (29). In (33) and in the following the prime in the sum denotes the omission of the contribution from $m = n = 0$. By performing either the sum over m or the sum over n in (33) one gets

$$\Gamma(c) = \sum_{n \geq 1} \frac{(-1)^n}{n} \frac{\cos(2n\pi c) - 1}{\text{sh}(n\pi\beta/2L)} \quad (34)$$

$$\Gamma(c) = \sum_{m \geq 1} \frac{(-1)^m}{m} \frac{\text{ch}(4m\pi c L/\beta) - 1}{\text{sh}(2m\pi L/\beta)} + \frac{2\pi L}{\beta} c^2 \quad (35)$$

both valid for $c \in [-1/2, 1/2]$ and periodically continued otherwise. These two equivalent forms will be useful in the low- and high- temperature expansion of the condensates.

2.6 Effective Action

The final step is to combine the classical (euclidean) action of the photon field, rewritten in the variables (11)

$$S_B[\phi] \equiv \frac{1}{4} F_{\mu\nu} F_{\mu\nu} = \frac{1}{2e^2} \Delta\phi\Delta\phi \quad (36)$$

with the result for the functional determinant (25). Collecting the contributions (27, 28) or (30, 31) as well as (34) or (35) and adding the classical action (36) one ends up with the effective action (which, of course, does not contain the gauge degree of freedom χ)

$$\Gamma \equiv \Gamma_{\theta, N_f}[c, \phi] \equiv N_f \cdot \Gamma(c) + \Gamma_{\theta, N_f}[\phi] \quad (37)$$

where $\Gamma(c)$ has been given in (34, 35) and $\Gamma_{\theta, N_f}[\phi]$ is

$$\Gamma_{\theta, N_f}[\phi] \equiv \frac{1}{2e^2} \left\{ \int \phi \Delta^2 \phi - \mu^2 \int \phi \Delta \phi + \mu^2 \cdot \theta \int \Delta \phi \right\} \quad (38)$$

where the fact that the functional determinant is the same for all flavours has been used. In (38) μ is the Schwinger mass (5) which is the analog of the η' -mass in 3-flavour-QCD.

In summary, the functional measure takes the form

$$d\mu_\theta[A] = \frac{1}{Z_\theta} e^{-\Gamma_{\theta, N_f}[c, \phi]} dc D\phi \delta(\chi) D\chi \quad (39)$$

where we have taken into account that the gauge-variation of the Lorentz gauge-condition $F := \partial_\mu A^\mu = \Delta\chi$ and the Jacobian of the transformation from $\{A\}$ to the variables $\{\phi, c, \chi\}$ are independent of the fields. Actually, the corresponding determinants cancel each other.

We conclude that the expectation-value of any gauge-invariant operator O (which will not depend on χ) is given by

$$\langle O \rangle = \frac{\int dc D\phi O e^{-\Gamma_{\theta, N_f}[c, \phi]}}{\int dc D\phi e^{-\Gamma_{\theta, N_f}[c, \phi]}} \quad (40)$$

with $\Gamma_{\theta, N_f}[c, \phi]$ given by (37, 38) and (34, 35).

3 Condensates in a Finite Volume

The general result (40) may be applied to calculate the chiral condensates

$$\langle \psi^\dagger(x) P_\pm \psi(x) \rangle = \frac{\int dc D\phi S_\theta(x, x)_{\pm\pm} e^{-\Gamma_{\theta, N_f}[c, \phi]}}{\int dc D\phi e^{-\Gamma_{\theta, N_f}[c, \phi]}} \quad (41)$$

with S_θ from (22) and Γ_θ from (37). Both the (exponentiated) action and the Green's function factorize into parts which only depend on c and ϕ , respectively. Thus (41) factorizes as

$$\langle \psi^\dagger(x) P_\pm \psi(x) \rangle = C^\pm(x) \cdot D^\pm(x) \quad (42)$$

with x^0 -independent factors

$$C^\pm(x^1) = \frac{\int dc \tilde{S}_\theta(x, x)_{\pm\pm} e^{-N_f \Gamma(c)}}{\int dc e^{-N_f \Gamma(c)}} \quad , \quad (43)$$

$$D^\pm(x^1) = \frac{\int D\phi e^{\mp 2\phi(x) - \Gamma_{\theta, N_f}[\phi]}}{\int D\phi e^{-\Gamma_{\theta, N_f}[\phi]}} \quad (44)$$

which depend on the parameters θ, N_f, β, L . Here and below the c -integrals extend over the period $[-1/2, 1/2]$, whereas the field ϕ is subject to Dirichlet boundary conditions at the two ends $x^1=0$ and $x^1=L$. The next step is to evaluate the factors C^\pm and D^\pm in (42) for given circumference β and length L of the cylinder and given values of θ and N_f .

3.1 Harmonic Integral

In order to evaluate the first factor in (42) it is worth noticing that the two forms (34, 35) allow one to write the factor $\exp\{-\Gamma(c)\}$ in the two equivalent versions

$$e^{-\Gamma(c)} = \frac{\theta_3(c, i\tau)}{\theta_3(0, i\tau)} \quad (45)$$

$$e^{-\Gamma(c)} = e^{-\pi c^2/\tau} \frac{\theta_3(ic/\tau, i/\tau)}{\theta_3(0, i/\tau)}. \quad (46)$$

Here we employed the notation

$$\theta_3(u, \omega) = \sum_{n \in \mathbb{Z}} e^{2\pi i n u} q^{n^2} = 1 + 2 \sum_{n \geq 1} \cos(2n\pi u) q^{n^2} \quad (q \equiv e^{i\pi\omega}) \quad (47)$$

for the parameters $\omega = i\tau$ and $\omega = i/\tau$ (giving real nome $q \in]0, 1[$) respectively. In deriving (45) and (46) we used the infinite-product expansion [22]

$$\theta_3(u, \omega) = \prod_{n \geq 1} (1 - q^{2n})(1 + 2q^{2n-1} \cos(2\pi u) + q^{2(2n-1)}) \quad (48)$$

and the addition theorem [23]

$$\ln \left(\frac{\theta_3(u+v, \omega)}{\theta_3(u-v, \omega)} \right) = 4 \sum_{n \geq 1} \frac{(-1)^n}{n} \frac{q^n}{1 - q^{2n}} \sin(2\pi n u) \sin(2\pi n v) \quad (49)$$

respectively. The Poisson resummation lemma makes sure that

$$\sum_{n \in \mathbb{Z}} e^{-(x+n)^2 \cdot t} = \sqrt{\pi/t} \sum_{n \in \mathbb{Z}} e^{-\pi^2 n^2/t} e^{2\pi i n x} \quad (x \in \mathbb{R}, t > 0) \quad (50)$$

from which we derive the theta-function duality relation

$$\sqrt{\tau} \theta_3(c, i\tau) = e^{-\pi c^2/\tau} \theta_3(\pm ic/\tau, i/\tau) \quad (c \in \mathbb{R}, \tau > 0) \quad (51)$$

which in turn allows to confirm the identity of the right-hand sides of (45) and (46).

Starting from expression (43) and plugging in the Green's function (20) as well as (45) or alternatively the Green's function (21) along with (46) one ends up with

$$C^\pm(x^1) = \pm \frac{e^{\pm\theta}}{4L} \sum_{n \in \mathbb{Z}} (-1)^n \frac{\sin(\pi\xi) \text{ch}(\pi n \tau)}{\sin^2(\pi\xi) + \text{sh}^2(\pi n \tau)} \cdot \frac{\int \cos(2\pi n c) \theta_3^{N_f}(c, i\tau) dc}{\int \theta_3^{N_f}(c, i\tau) dc} \quad (52)$$

$$C^\pm(x^1) = \pm \frac{e^{\pm\theta}}{2\beta} \sum_{m \in \mathbb{Z}} (-1)^m \frac{1}{\text{sh}(\pi(m+\xi)/\tau)} \cdot \frac{\int \text{ch}(2\pi(m+\xi)c/\tau) e^{-N_f \pi c^2/\tau} \theta_3^{N_f}(ic/\tau, i/\tau) dc}{\int e^{-N_f \pi c^2/\tau} \theta_3^{N_f}(ic/\tau, i/\tau) dc} \quad (53)$$

which is independent of x^0 as required by translation-invariance. In the last step we have taken advantage from the fact that $\theta_3(., .)$ is symmetric in its first argument and the c -integration is from $-1/2$ to $1/2$.

3.2 Scalar Integral

For the evaluation of the second factor in (42) we recall that the integration extends over fields ϕ which are periodic in the x^0 and satisfy Dirichlet boundary-conditions at $x^1 = 0, L$. The first thing to do is to perform the gaussian integrals to get (Δ' is the Laplacian taking derivatives w.r.t. x')

$$D^\pm(x^1) = \exp \left\{ \frac{2\pi}{N_f} K(x, x) \right\} \cdot \exp \left\{ \pm \frac{\theta}{2} \cdot \int \Delta' K(x, x') d^2 x' \pm \frac{\theta}{2} \cdot \int \Delta' K(x', x) d^2 x' \right\} \quad (54)$$

where the integration is over x' and the kernel (employing the Schwinger mass (5))

$$K(x, y) = \langle x | \frac{\mu^2}{-\Delta(-\Delta + \mu^2)} | y \rangle = \langle x | \frac{1}{-\Delta} | y \rangle - \langle x | \frac{1}{-\Delta + \mu^2} | y \rangle \quad (55)$$

is with respect to Dirichlet boundary conditions. From its explicit form one finds [17]

$$K(x, x) = \frac{1}{2\pi} \sum_{n \geq 1} \left(1 - \cos(2n\pi\xi) \right) \left(\frac{\text{cth}(n\pi\tau)}{n} - (n \rightarrow \sqrt{n^2 + (\mu L/\pi)^2}) \right) \quad (56)$$

$$K(x, x) = \frac{\xi(1-\xi)}{2\tau} + \frac{\text{ch}(\mu L(1-2\xi)) - \text{ch}(\mu L)}{2\mu\beta \text{sh}(\mu L)} + \frac{1}{2\pi} \sum_{m \geq 1} \frac{\text{ch}(m\pi/\tau) - \text{ch}(m\pi(1-2\xi)/\tau)}{m \text{sh}(m\pi/\tau)} - (m \rightarrow \sqrt{m^2 + (\mu\beta/2\pi)^2}) \quad (57)$$

which is perfectly finite as well as

$$\int \Delta' K(x, x') d^2 x' = \int \Delta' K(x', x) d^2 x' = \frac{\text{sh}(\mu L(1-\xi)) + \text{sh}(\mu L\xi)}{\text{sh}(\mu L)} - 1 \quad (58)$$

from which the factor (54) can be computed. As one can see, all three expressions (56, 57, 58) tend to zero as x approaches the boundary. The result for (54) is then found to read

$$D^\pm(x^1) = \exp \left\{ \frac{1}{N_f} \sum_{n \geq 1} \left(1 - \cos(2n\pi\xi) \right) \left(\frac{\text{cth}(n\pi\tau)}{n} - (n \rightarrow \sqrt{n^2 + (\mu L/\pi)^2}) \right) \right\} \cdot \exp \left\{ \pm \theta \cdot \left(\frac{\text{sh}(\mu L(1-\xi)) + \text{sh}(\mu L\xi)}{\text{sh}(\mu L)} - 1 \right) \right\} \quad (59)$$

$$D^\pm(x^1) = \exp \left\{ \frac{2\pi}{N_f} \left(\frac{\xi(1-\xi)}{2\tau} + \frac{\text{ch}(\mu L(1-2\xi)) - \text{ch}(\mu L)}{2\mu\beta \text{sh}(\mu L)} \right) \right\} \cdot \exp \left\{ \frac{1}{N_f} \sum_{m \geq 1} \frac{\text{ch}(m\pi/\tau) - \text{ch}(m\pi(1-2\xi)/\tau)}{m \text{sh}(m\pi/\tau)} - (m \rightarrow \sqrt{m^2 + (\mu\beta/2\pi)^2}) \right\} \cdot \exp \left\{ \pm \theta \cdot \left(\frac{\text{sh}(\mu L(1-\xi)) + \text{sh}(\mu L\xi)}{\text{sh}(\mu L)} - 1 \right) \right\} \quad (60)$$

which is independent of x^0 as required by translation-invariance.

3.3 Analytical Expression for Condensate at Arbitrary Points

The chiral condensate (42) is simply the product of (52) and (59) or equivalently (53) and (60). Rescaled by natural units (4), it takes the form

$$\frac{\langle \psi^\dagger P_\pm \psi \rangle(x^1)}{(|e|/\sqrt{\pi})} = \pm \frac{e^{\pm\theta \cdot \text{ch}(\lambda\sqrt{N_f}(1-2\xi)/2)/\text{ch}(\lambda\sqrt{N_f}/2)}}{4\lambda} \cdot \sum_{n \in \mathbb{Z}} (-1)^n \frac{\sin(\pi\xi)\text{ch}(\pi n\tau)}{\sin^2(\pi\xi) + \text{sh}^2(\pi n\tau)} \cdot \frac{\int \cos(2\pi n c) \theta_3^{N_f}(c, i\tau) dc}{\int \theta_3^{N_f}(c, i\tau) dc} \cdot \exp \left\{ \frac{1}{N_f} \sum_{n \geq 1} \left(1 - \cos(2n\pi\xi) \right) \left(\frac{\text{cth}(n\pi\tau)}{n} - (n \rightarrow \sqrt{n^2 + N_f(\lambda/\pi)^2}) \right) \right\} \quad (61)$$

$$\begin{aligned}
\frac{\langle \psi^\dagger P_\pm \psi \rangle(x^1)}{(|e|/\sqrt{\pi})} &= \pm \frac{e^{\pm\theta \cdot \text{ch}(\lambda\sqrt{N_f}(1-2\xi)/2)/\text{ch}(\lambda\sqrt{N_f}/2)}}{2\sigma} \cdot \\
&\sum_{m \in \mathbb{Z}} (-1)^m \frac{1}{\text{sh}(\pi(m+\xi)/\tau)} \cdot \frac{\int \text{ch}(2\pi(m+\xi)c/\tau) e^{-N_f \pi c^2/\tau} \theta_3^{N_f}(ic/\tau, i/\tau) dc}{\int e^{-N_f \pi c^2/\tau} \theta_3^{N_f}(ic/\tau, i/\tau) dc} \cdot \\
&\exp \left\{ \frac{\pi}{N_f} \left(\frac{\xi(1-\xi)}{\tau} + \frac{\text{ch}(\lambda\sqrt{N_f}(1-2\xi)) - \text{ch}(\lambda\sqrt{N_f})}{\sigma\sqrt{N_f} \text{sh}(\lambda\sqrt{N_f})} \right) \right\} \cdot \quad (62) \\
&\exp \left\{ \frac{1}{N_f} \sum_{m \geq 1} \frac{\text{ch}(m\pi/\tau) - \text{ch}(m\pi(1-2\xi)/\tau)}{m \text{sh}(m\pi/\tau)} - (m \rightarrow \sqrt{m^2 + N_f(\sigma/2\pi)^2}) \right\}
\end{aligned}$$

where the ξ -independent but θ -dependent parts of the two factors have cancelled. Note that the two forms (61) and (62) are identical for any finite (dimensionless) lengths σ and λ , but enjoy excellent convergence properties in the low- ($\tau \gg 1$) and high- ($\tau \ll 1$) temperature regimes, respectively.

4 Numerical Evaluation for $N_f = 1$ and $N_f = 2$

The general result (61, 62) shall be specialized to the cases $N_f = 1$ and $N_f = 2$ as the integration over c can be done in these cases. The aim is to collect specific observations concerning the difference between the single-flavour and multi-flavour case.

4.1 Specialization to $N_f = 1$ at Arbitrary Points

For one flavour the c -integrals in (61, 62) can be performed. Taking into account the fact that they extend over the interval $[-1/2, 1/2]$ the result is found to read

$$\begin{aligned}
\frac{\langle \psi^\dagger P_\pm \psi \rangle}{(|e|/\sqrt{\pi})} &= \pm \frac{e^{\pm\theta \cdot \text{ch}(\lambda/2 - \lambda\xi)/\text{ch}(\lambda/2)}}{4\lambda} \sum_{n \in \mathbb{Z}} (-1)^n \frac{\sin(\pi\xi) \text{ch}(\pi n \tau)}{\sin^2(\pi\xi) + \text{sh}^2(\pi n \tau)} \exp(-n^2 \pi \tau) \cdot \\
&\exp \left\{ \sum_{n \geq 1} \left(1 - \cos(2n\pi\xi) \right) \left(\frac{\text{cth}(n\pi\tau)}{n} - (n \rightarrow \sqrt{n^2 + (\lambda/\pi)^2}) \right) \right\} \quad (63)
\end{aligned}$$

$$\begin{aligned}
\frac{\langle \psi^\dagger P_\pm \psi \rangle}{(|e|/\sqrt{\pi})} &= \pm \frac{e^{\pm\theta \cdot \text{ch}(\lambda/2 - \lambda\xi)/\text{ch}(\lambda/2)}}{2\sigma} \sum_{m \in \mathbb{Z}} (-1)^m \frac{1}{\text{sh}(\pi(m+\xi)/\tau)} \times \\
&\frac{\sum_{k \in \mathbb{Z}} e^{\pi(m+\xi)(2k+m+\xi)/\tau} (\text{erf}(\frac{(k+m+\xi+1/2)\sqrt{\pi}}{\sqrt{\tau}}) - \text{erf}(\frac{(k+m+\xi-1/2)\sqrt{\pi}}{\sqrt{\tau}}))}{2} \cdot \\
&\exp \left\{ \pi \left(\frac{\xi(1-\xi)}{\tau} + \frac{\text{ch}(\lambda(1-2\xi)) - \text{ch}(\lambda)}{\sigma \text{sh}(\lambda)} \right) \right\} \cdot \\
&\exp \left\{ \sum_{m \geq 1} \frac{\text{ch}(m\pi/\tau) - \text{ch}(m\pi(1-2\xi)/\tau)}{m \text{sh}(m\pi/\tau)} - (m \rightarrow \sqrt{m^2 + (\sigma/2\pi)^2}) \right\} \quad (64)
\end{aligned}$$

where again the two equivalent representations (63) and (64) enjoy excellent convergence properties in the low- ($\tau \gg 1$) and high- ($\tau \ll 1$) temperature regimes, respectively.

4.2 Specialization to $N_f = 2$ at Arbitrary Points

For two flavours the c -integrals in (61, 62) can be performed. Taking into account the fact that they extend over the interval $[-1/2, 1/2]$ the result is found to read

$$\frac{\langle \psi^\dagger P_\pm \psi \rangle}{(|e|/\sqrt{\pi})} = \pm \frac{e^{\pm\theta \cdot \text{ch}(\lambda/\sqrt{2} - \sqrt{2}\lambda\xi)/\text{ch}(\lambda/\sqrt{2})}}{4\lambda} \sum_{n \in \mathbb{Z}} (-1)^n \frac{\sin(\pi\xi) \text{ch}(\pi n\tau)}{\sin^2(\pi\xi) + \text{sh}^2(\pi n\tau)} \frac{\sum_{k \in \mathbb{Z}} e^{-(k^2 + (n-k)^2)\pi\tau}}{\sum_{k \in \mathbb{Z}} e^{-2k^2\pi\tau}} \cdot \exp \left\{ \frac{1}{2} \sum_{n \geq 1} (1 - \cos(2n\pi\xi)) \left(\frac{\text{cth}(n\pi\tau)}{n} - (n \rightarrow \sqrt{n^2 + 2(\lambda/\pi)^2}) \right) \right\} \quad (65)$$

$$\frac{\langle \psi^\dagger P_\pm \psi \rangle}{(|e|/\sqrt{\pi})} = \pm \frac{e^{\pm\theta \cdot \text{ch}(\lambda/\sqrt{2} - \sqrt{2}\lambda\xi)/\text{ch}(\lambda/\sqrt{2})}}{2\sigma} \sum_{m \in \mathbb{Z}} (-1)^m \frac{1}{\text{sh}(\pi(m + \xi)/\tau)} \times \frac{\sum_{q \in \mathbb{Z}} \sum_{p \in \mathbb{Z}} \frac{1 + (-1)^{p+q}}{2} e^{\pi((p+m+\xi)^2 - p^2 - q^2)/2\tau} (\text{erf}(\frac{(p+m+\xi+1)\sqrt{\pi}}{\sqrt{2\tau}}) - \text{erf}(\frac{(p+m+\xi-1)\sqrt{\pi}}{\sqrt{2\tau}}))}{2 \sum_{q \in \mathbb{Z}} e^{-\pi q^2/2\tau}} \cdot \exp \left\{ \frac{\pi}{2} \left(\frac{\xi(1-\xi)}{\tau} + \frac{\text{ch}(\sqrt{2}\lambda(1-2\xi)) - \text{ch}(\sqrt{2}\lambda)}{\sqrt{2}\sigma \text{sh}(\sqrt{2}\lambda)} \right) \right\} \cdot \exp \left\{ \frac{1}{2} \sum_{m \geq 1} \frac{\text{ch}(m\pi/\tau) - \text{ch}(m\pi(1-2\xi)/\tau)}{m \text{sh}(m\pi/\tau)} - (m \rightarrow \sqrt{m^2 + 2(\sigma/2\pi)^2}) \right\} \quad (66)$$

where again the two equivalent representations (65) and (66) enjoy excellent convergence properties in the low- ($\tau \gg 1$) and high- ($\tau \ll 1$) temperature regimes, respectively.

4.3 Numerical Evaluation of ξ -Dependence

We are now in a position to evaluate formulas (63,64) for $N_f = 1$ as well as formulas (65,66) for $N_f = 2$. The first hint regarding the difference between single-flavour and multi-flavour cases might come from observing how the spatial dependence of the condensate behaves as temperature and box-length vary. Since the condensate diverges on the boundaries as ξ^{-1} and $(1 - \xi)^{-1}$ respectively ¹, it is the quantity $4\xi(1 - \xi)|\langle \psi^\dagger P_\pm \psi \rangle|/(|e|/\sqrt{\pi})$ at $\theta = 0$ which is displayed in figures 2 and 3.

From inspecting figures 2 and 3 one is lead to the observation that for any finite temperature the condensate ends up “creeping into the boundaries” (and fading away at any internal point of the box) once the box-length is sufficiently large.

On the other hand, cooling the system seems to have the opposite effect, i.e. to a first approximation, the shape of the spatial distribution of the condensate seems to depend on the ratio $\tau = \sigma/2\lambda$. However, as σ and λ both tend to be large, the spatial distribution starts to look qualitatively different in the two cases $N_f = 1$ and $N_f = 2$, respectively. This is a pictorial hint indicating a difference between the single-flavour and the multi-flavour versions of the model once the twofold limit $\sigma \rightarrow \infty, \lambda \rightarrow \infty$ is performed.

¹There is no reason to start worrying: On the boundary the field has to satisfy a boundary condition which lets the free Green’s function take the form given in (19). This expression stays finite as one of its two entries $-x$ or y reaches the boundary but not if x and y reach the same point on the boundary, which simply means that there is no consistent double-boundary solution.

Figure 2: Spatial Dependence of $4\xi(1-\xi)|\langle\psi^\dagger P_{\pm}\psi\rangle|/\mu_1$ for $N_f = 1$ ($\xi = x^1/L$).

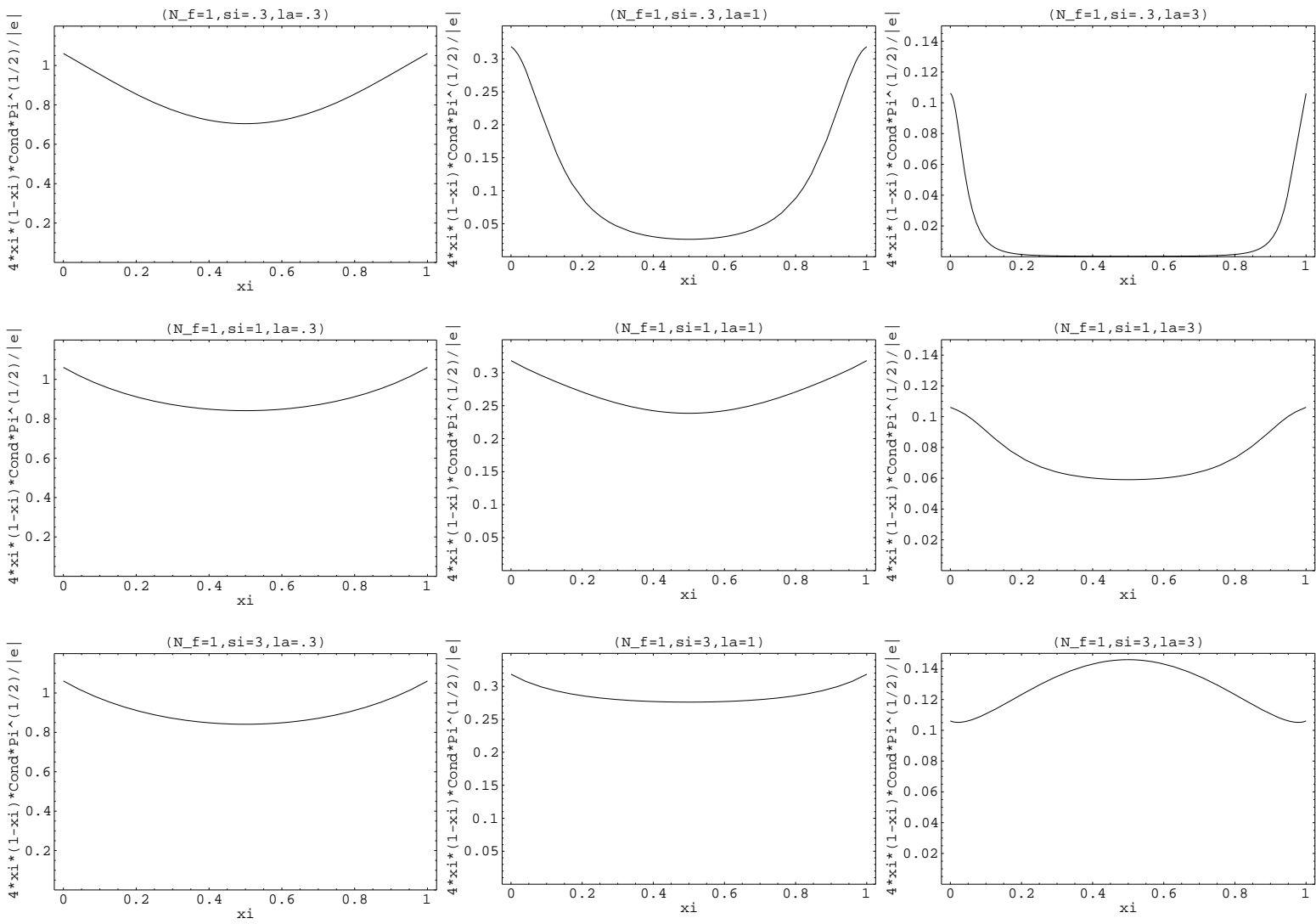
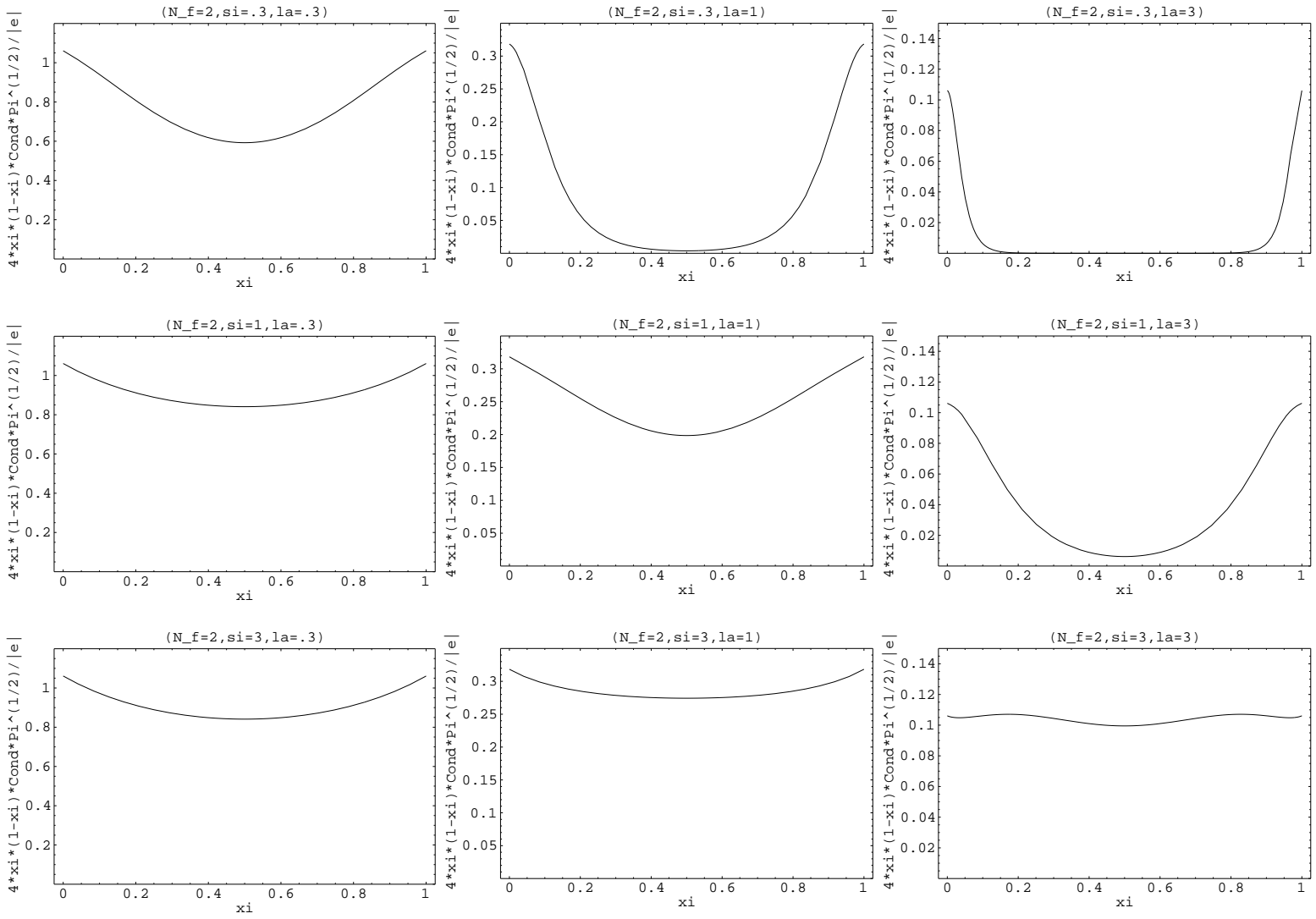


Figure 3: Spatial Dependence of $4\xi(1-\xi)|\langle\psi^\dagger P_{\pm}\psi\rangle|/\mu_1$ for $N_f = 2$ ($\xi = x^1/L$).



4.4 Specialization to $N_f = 1$ at Midpoints

As one concentrates on the midpoints ($\xi = 1/2$), formulae (63) and (64) take the form

$$\begin{aligned} \frac{\langle \psi^\dagger P_\pm \psi \rangle}{(|e|/\sqrt{\pi})} &= \pm \frac{e^{\pm\theta/\text{ch}(\lambda/2)}}{4\pi} \left(1 + 2 \sum_{n \geq 1} (-1)^n \frac{1}{\text{ch}(n\pi\tau)} \exp(-n^2\pi\tau) \right) \cdot \\ &\quad \exp \left\{ \gamma - 2 \sum_{j \geq 1} (-1)^j K_0(j\lambda) \right\} \\ &\quad \exp \left\{ 4 \sum_{n \geq 0} \frac{1}{(2n+1)(e^{2(2n+1)\pi\tau} - 1)} - ((2n+1) \rightarrow \sqrt{(2n+1)^2 + (\lambda/\pi)^2}) \right\} \end{aligned} \quad (67)$$

$$\begin{aligned} \frac{\langle \psi^\dagger P_\pm \psi \rangle}{(|e|/\sqrt{\pi})} &= \pm \frac{e^{\pm\theta/\text{ch}(\lambda/2)}}{4\pi} \sum_{m \geq 0} (-1)^m \frac{e^{-\pi((2m+1)^2-1)/4\tau}}{\text{sh}(\pi(2m+1)/2\tau)} \times \\ &\quad \sum_{k \geq 0} \text{ch}\left(\frac{\pi(2m+1)(2k+1)}{2\tau}\right) \left(\text{erf}\left(\frac{(k+1)\sqrt{\pi}}{\sqrt{\tau}}\right) - \text{erf}\left(\frac{k\sqrt{\pi}}{\sqrt{\tau}}\right) \right) \cdot \\ &\quad \exp \left\{ \gamma + \frac{\pi(1 - \text{th}(\lambda/2))}{\sigma} - 2 \sum_{j \geq 1} K_0(j\sigma) \right\} \cdot \\ &\quad \exp \left\{ -2 \sum_{m \geq 1} \frac{1}{m(e^{m\pi/\tau} + 1)} - (m \rightarrow \sqrt{m^2 + (\sigma/2\pi)^2}) \right\} \end{aligned} \quad (68)$$

respectively (for details, see appendix), from which we derive

$$\lim_{\sigma \rightarrow \infty} \frac{\langle \psi^\dagger P_\pm \psi \rangle(\frac{L}{2})}{(|e|/\sqrt{\pi})} = \pm \frac{e^{\pm\theta/\text{ch}(\lambda/2)}}{4\pi} \exp \left\{ \gamma - 2 \sum_{j \geq 1} (-1)^j K_0(j\lambda) \right\} \quad (69)$$

$$\lim_{\lambda \rightarrow \infty} \frac{\langle \psi^\dagger P_\pm \psi \rangle(\frac{L}{2})}{(|e|/\sqrt{\pi})} = \pm \frac{1}{4\pi} \exp \left\{ \gamma - 2 \sum_{j \geq 1} K_0(j\sigma) \right\} \quad (70)$$

for $N_f = 1$. Thus

$$\lim_{\lambda \rightarrow \infty} \lim_{\sigma \rightarrow \infty} \frac{\langle \psi^\dagger P_\pm \psi \rangle(\frac{L}{2})}{(|e|/\sqrt{\pi})} = \pm \frac{1}{4\pi} e^\gamma = \lim_{\sigma \rightarrow \infty} \lim_{\lambda \rightarrow \infty} \frac{\langle \psi^\dagger P_\pm \psi \rangle(\frac{L}{2})}{(|e|/\sqrt{\pi})} \quad (71)$$

for $N_f = 1$. Note that (70) and the second equality in (71) correct for an erroneous result in [17] which was won by performing the limit under the c -integral.

4.5 Specialization to $N_f = 2$ at Midpoints

As one concentrates on the midpoints ($\xi = 1/2$), formulae (65) and (66) take the form

$$\begin{aligned} \frac{\langle \psi^\dagger P_\pm \psi \rangle}{(|e|/\sqrt{\pi})} &= \pm \frac{2^{1/4} e^{\pm\theta/\text{ch}(\lambda/\sqrt{2})}}{4\sqrt{\pi} \sqrt{\lambda}} \cdot \\ &\quad \left(1 + 2 \sum_{n \geq 1} (-1)^n \frac{e^{-n^2\pi\tau/2}}{\text{ch}(n\pi\tau)} \cdot \frac{e^{-n^2\pi\tau/2} + 2 \sum_{k \geq 1} \frac{e^{-(n/2-k)^2 2\pi\tau} + e^{-(n/2+k)^2 2\pi\tau}}{2}}{1 + 2 \sum_{k \geq 1} e^{-2k^2\pi\tau}} \right) \cdot \end{aligned}$$

$$\exp\left\{\frac{\gamma}{2} - \sum_{j \geq 1} (-1)^j K_0(j\sqrt{2}\lambda)\right\}$$

$$\exp\left\{2 \sum_{n \geq 0} \frac{1}{(2n+1)(e^{2(2n+1)\pi\tau} - 1)} - ((2n+1) \rightarrow \sqrt{(2n+1)^2 + 2(\lambda/\pi)^2})\right\} \quad (72)$$

$$\frac{\langle \psi^\dagger P_\pm \psi \rangle}{(|e|/\sqrt{\pi})} = \pm \frac{2^{1/4} e^{\pm\theta/\text{ch}(\lambda/\sqrt{2})}}{4\sqrt{\pi} \sqrt{\sigma}} \sum_{m \geq 0} (-1)^m \frac{e^{-\pi((2m+1)^2-1)/8\tau}}{\text{sh}(\pi(2m+1)/2\tau)} \times$$

$$\frac{\sum_{q \in Z} e^{-\pi q^2/2\tau} \sum_{p \geq 0} \text{ch}\left(\frac{\pi(p+1/2)(m+1/2)}{\tau}\right) (\text{erf}\left(\frac{p+3/2}{\sqrt{2\tau/\pi}}\right) - \text{erf}\left(\frac{p-1/2}{\sqrt{2\tau/\pi}}\right)) + \sum_{q \in Z} e^{-\pi q^2/2\tau} \sum_{p \geq 0} (-1)^{p+q-m} \text{sh}\left(\frac{\pi(p+1/2)(m+1/2)}{\tau}\right) (\text{erf}\left(\frac{p+3/2}{\sqrt{2\tau/\pi}}\right) - \text{erf}\left(\frac{p-1/2}{\sqrt{2\tau/\pi}}\right))}{\sum_{q \in Z} e^{-\pi q^2/2\tau}}$$

$$\exp\left\{\frac{\gamma}{2} + \frac{\pi(1-\text{th}(\lambda/\sqrt{2}))}{2\sqrt{2}\sigma} - \sum_{j \geq 1} K_0(j\sqrt{2}\sigma)\right\}$$

$$\exp\left\{-\sum_{m \geq 1} \frac{1}{m(e^{\pi m/\tau} + 1)} - (m \rightarrow \sqrt{m^2 + 2(\sigma/2\pi)^2})\right\} \quad (73)$$

respectively (for details, see appendix), from which we derive

$$\lim_{\sigma \rightarrow \infty} \frac{\langle \psi^\dagger P_\pm \psi \rangle(\frac{L}{2})}{(|e|/\sqrt{\pi})} = \pm \frac{2^{1/4} e^{\pm\theta/\text{ch}(\lambda/\sqrt{2})}}{4\sqrt{\pi} \sqrt{\lambda}} \exp\left\{\frac{\gamma}{2} - \sum_{j \geq 1} (-1)^j K_0(j\sqrt{2}\lambda)\right\} \quad (74)$$

$$\lim_{\lambda \rightarrow \infty} \frac{\langle \psi^\dagger P_\pm \psi \rangle(\frac{L}{2})}{(|e|/\sqrt{\pi})} = 0 \quad (75)$$

for $N_f = 2$. Thus

$$\lim_{\lambda \rightarrow \infty} \lim_{\sigma \rightarrow \infty} \frac{\langle \psi^\dagger P_\pm \psi \rangle(\frac{L}{2})}{(|e|/\sqrt{\pi})} = 0 = \lim_{\sigma \rightarrow \infty} \lim_{\lambda \rightarrow \infty} \frac{\langle \psi^\dagger P_\pm \psi \rangle(\frac{L}{2})}{(|e|/\sqrt{\pi})} \quad (76)$$

for $N_f = 2$. Note that in the first case the condensate decays rather reluctantly ($\propto 1/\sqrt{\lambda}$) only under the outer limit, whereas in the second case it decays exponentially fast under the inner limit already (see appendix). This difference may be stated in equations through

$$\lim_{\lambda \rightarrow \infty} \lim_{\sigma \rightarrow \infty} \sqrt{\lambda} \frac{\langle \psi^\dagger P_\pm \psi \rangle(\frac{L}{2})}{(|e|/\sqrt{\pi})} = \pm \frac{2^{1/4}}{4\sqrt{\pi}} \exp\left\{\frac{\gamma}{2}\right\} \quad (77)$$

$$\lim_{\sigma \rightarrow \infty} \lim_{\lambda \rightarrow \infty} \sqrt{\lambda} \frac{\langle \psi^\dagger P_\pm \psi \rangle(\frac{L}{2})}{(|e|/\sqrt{\pi})} = 0 \quad (78)$$

which is peculiar for $N_f = 2$.

4.6 Numerical Evaluation at Midpoints

We are now in a position to numerically evaluate formulas (67, 68) for $N_f = 1$ as well as formulas (72, 73) for $N_f = 2$.

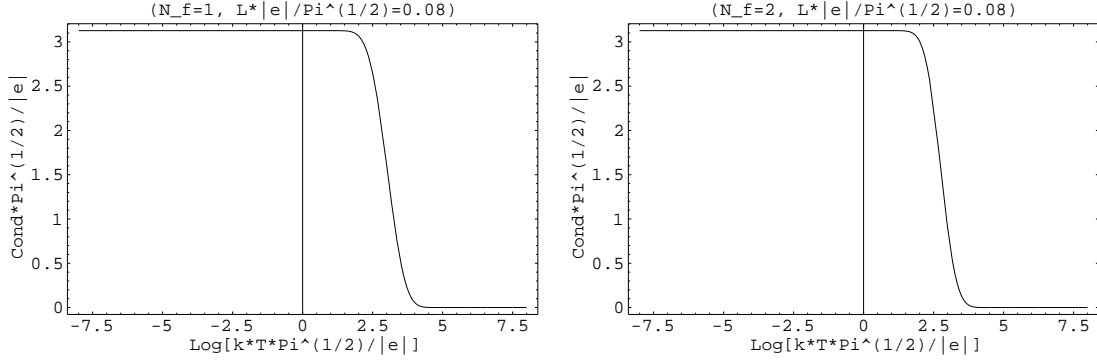


Figure 4: $|\langle \psi^\dagger P_\pm \psi \rangle|/\mu_1$ as a function of $\log(kT/\mu_1)$ at $L = 0.08/\mu_1$ for $N_f = 1$ and $N_f = 2$.

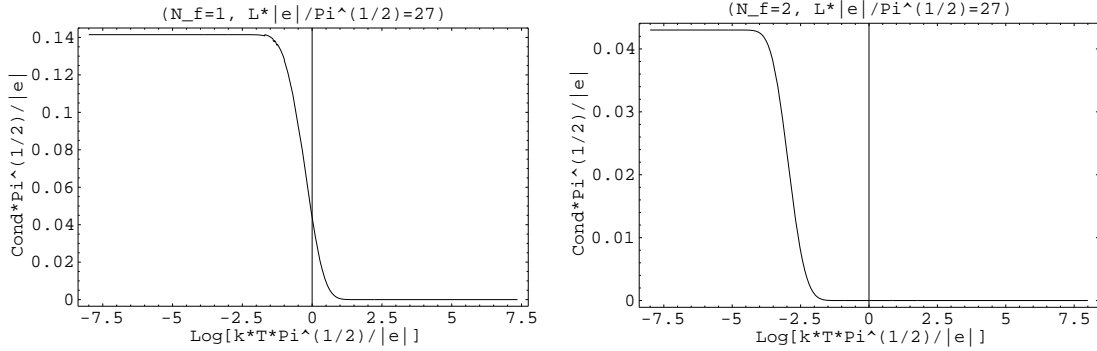


Figure 5: $|\langle \psi^\dagger P_\pm \psi \rangle|/\mu_1$ as a function of $\log(kT/\mu_1)$ at $L = 27.0/\mu_1$ for $N_f = 1$ and $N_f = 2$.

The following figures display the absolute value of the condensate at $\theta = 0$ in the center of the box. The two-dimensional graphs show the condensate as a function of $\sigma = \beta \cdot |e|/\pi^{1/2}$ (or a function thereof) at fixed value of $\lambda = L \cdot |e|/\pi^{1/2}$. Throughout we use $\mu_1 = |e|/\pi^{1/2}$. The surface- and density-plots show the condensate versus (a function of) σ and λ .

It might be worth mentioning that in each of those figures both representations – (82) and (84) in case of $N_f = 1$ as well (86) and (87) in case of $N_f = 2$ – were used, the former formulas got evaluated for low temperatures ($\tau \gg 1$), the latter ones got evaluated for high temperatures ($\tau \ll 1$) — the switching being done in the region of the crossover transition, which essentially gives a numerical check that the representations (82) and (84) as well as the representations (86) and (87) indeed might be identical.

From figures 4 and 5 the system is seen to undergo a surprisingly well-localized crossover, which – however – doesn’t meet the criteria for a phase-transition of whatever kind as it is arbitrarily smooth (i.e. $\in C^\infty$).

By comparing figures 4 and 5, one realizes that increasing the box-length essentially moves the “kink” to the left, i.e. increasing the box-length results in a decrease of the “critical temperature” (the effect being much stronger in case $N_f = 2$ than for $N_f = 1$) and one starts wondering whether this kink-phenomenon survives the limit $L \rightarrow \infty$. We will see that the answer to this question depends in a critical way on the number of flavours; the two cases $N_f = 1$ and $N_f = 2$ turn out to be different. The “plateaus” seem to be equally high for one and two flavours as long as the box-length is small (cf. figure 4) but the height of the plateau decreases unequally rapidly if the box-length is increased (cf. figure 5 – compare the scales!).

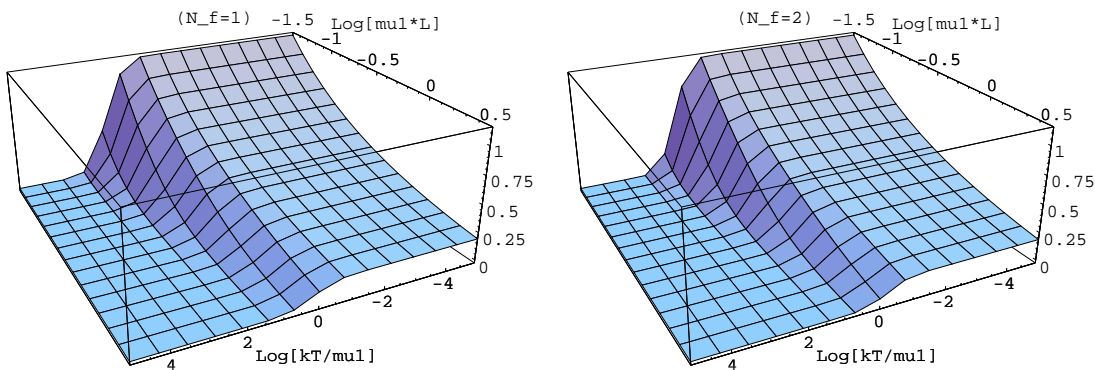


Figure 6: $|\langle\psi^\dagger P_\pm\psi\rangle|/\mu_1$ as a function of $\log(kT/\mu_1)$ and $\log(L\mu_1)$ for $N_f = 1$ and $N_f = 2$.

In order to reach an intuitive understanding it is worth having a look at figure 6. Thereby one realizes that there is a considerable fraction of the $\log(kT/\mu_1)$ - $\log(L\mu_1)$ -plane where the condensate is exponentially close (but not equal) to zero. Thus it might be helpful to introduce the concept of a *quasi-phase* with *almost* restored chiral symmetry. In order to do so one has to decide on a trigger-value which the condensate has to exceed in order to constitute a point (in the $\log(kT/\mu_1)$ - $\log(L\mu_1)$ -plane) with manifestly broken symmetry. While this choice is – in principle – arbitrary, it seems natural to agree on half of the classical value of the condensate in the original (one-flavour) Schwinger model as the discriminator which makes the distinction between the two “quasi-phases”. Numerically, it is about 0.07.

Doing so results in generating the two contour-plots in figure 7: White points are those which satisfy the criterion $|\langle\psi^\dagger P_\pm\psi\rangle| \geq e^\gamma \sqrt{e^2/\pi}/8\pi$ – they constitute the (quasi-)phase with *manifestly broken symmetry*. Black points are those which satisfy the criterion $|\langle\psi^\dagger P_\pm\psi\rangle| \leq e^\gamma \sqrt{e^2/\pi}/8\pi$ – they constitute the quasi-phase with *quasi-restored symmetry*. These two quasi-phases are separated by a “crossover-line” which essentially corresponds to the “border” of the zero-level plane in figure 6. In the form shown in figure 7 the concept of quasi-phases proves useful as it clearly shows in which areas of parameterspace the cases $N_f = 1$ and $N_f = 2$ seem to be similar and in which areas each of them shows a clearly distinct behaviour.

First we notice that the point $\beta = L = 0$ (lower right corner in figure 7) seems to lie close to or right on the crossover-line in either case $N_f = 1$ and $N_f = 2$ (note that data near the boundaries are cut off for numerical reasons). This observation lets us go back to formulas (61) and (62) and derive the (moderately interesting) noncommutativity-phenomenon

$$\lim_{L \rightarrow 0} \lim_{\beta \rightarrow 0} \langle\psi^\dagger P_\pm\psi\rangle\left(\frac{L}{2}\right) = 0 \quad (\forall N_f) \quad (79)$$

$$\lim_{\beta \rightarrow 0} \lim_{L \rightarrow 0} \langle\psi^\dagger P_\pm\psi\rangle\left(\frac{L}{2}\right) = \infty \quad (\forall N_f) \quad (80)$$

which is universal for any number of flavours.

Second we notice that the point $\beta = L = \infty$ (upper left corner in figure 7) definitely belongs to the manifestly broken (pseudo-) phase for $N_f = 1$ (l.h.s. of figure 7), but for $N_f = 2$ (r.h.s. of figure 7) the point $\beta = L = \infty$ seems either to be part of the quasi-phase with almost restored symmetry or to lie right on the crossover-line (note, again, that areas close to the boundaries in figure 7 are cut off for numerical reasons). This observation lets us try to zoom into the upper left corner in these quasi-phase-structure plots – an attempt which results in figure 8.

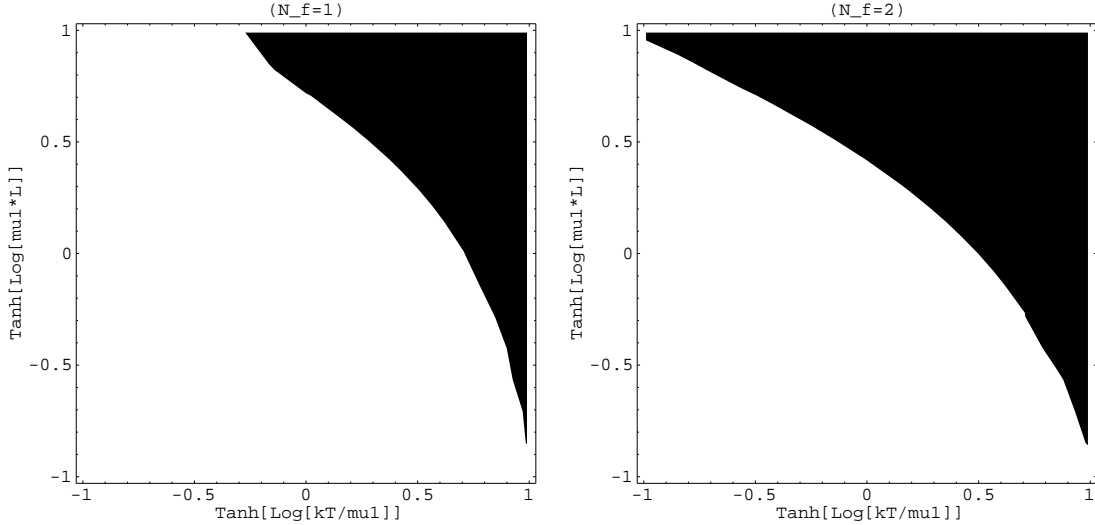


Figure 7: Quasi-Phasestructure as a function of $\log(kT/\mu_1)$ and $\log(L\mu_1)$ for $N_f = 1$ and $N_f = 2$, respectively. Definition: see text.

From the l.h.s. of figure 8 we learn that the one-flavour-system approaches its standard-value for the order-parameter in a very unspectacular way: The “classical” value for the condensate in the single-flavour model represents a plateau which is reached smoothly from any side. From the r.h.s. of figure 8 we learn that the two-flavour-system behaves in the large- L -limit in a way which depends rather sensitively on whether the temperature is exactly zero or finite: For any finite temperature the limiting value (zero) is approached smoothly (a statement which extends to the first derivative of the condensate), whereas at zero temperature the condensate seems to display a “square-root type” behaviour (as a function of $1/\lambda$). This is exactly what was predicted by formulas (74, 75): At zero temperature the two-flavour condensate goes to zero under $\lambda \rightarrow \infty$ – but only very reluctantly: $\propto 1/\sqrt{\lambda}$ (up to exponentially small corrections). On the other hand, for any fixed finite temperature, both the the condensate and its first derivative w.r.t. $1/\lambda$ vanish exponentially fast under $\lambda \rightarrow \infty$.

4.7 The order of the phase-transition at $T_c=0$

The statement that in the two-flavour model the behaviour of the chiral condensate as a function of $\lambda = \mu_1 L$ depends in a very sensitive way on whether $\sigma = \mu_1 \beta$ is finite or infinite turns out to be so crucial in the following that one would particularly welcome some further numerical evidence that there is, indeed, a “square-root type” behaviour of the condensate for $1/\lambda \ll 1$ at $1/\sigma=0$ (as opposed to a smooth behaviour for $\lambda \rightarrow \infty$ at $1/\sigma > 0$).

Though there is, quite generally, no numerical proof for smoothness, strong numerical evidence can be given that the boundary associated to $T=0$ of the two-flavour condensate surface in the r.h.s. of figure 8 does not just look like a square-root but, indeed, asymptotically gets a square-root and that this small- $1/\lambda$ -behaviour is, indeed, specific for $T=0$. To this end we simply decide to plot, for the two-flavour system, the quantity $2^{7/4} \pi^{1/2} e^{-\gamma} \cdot \sqrt{\lambda} |\langle \psi^\dagger P_\pm \psi \rangle| / \mu_1$, i.e. to include a factor $\propto \sqrt{\lambda}$. The result is shown in the r.h.s. of figure 9: the $T=0$ -boundary tends to 1 whereas the $1/L = \infty$ -boundary seems to be compatible with 0. In summary, the r.h.s. of figure 9 provides an independent numerical check of the analytical work (presented

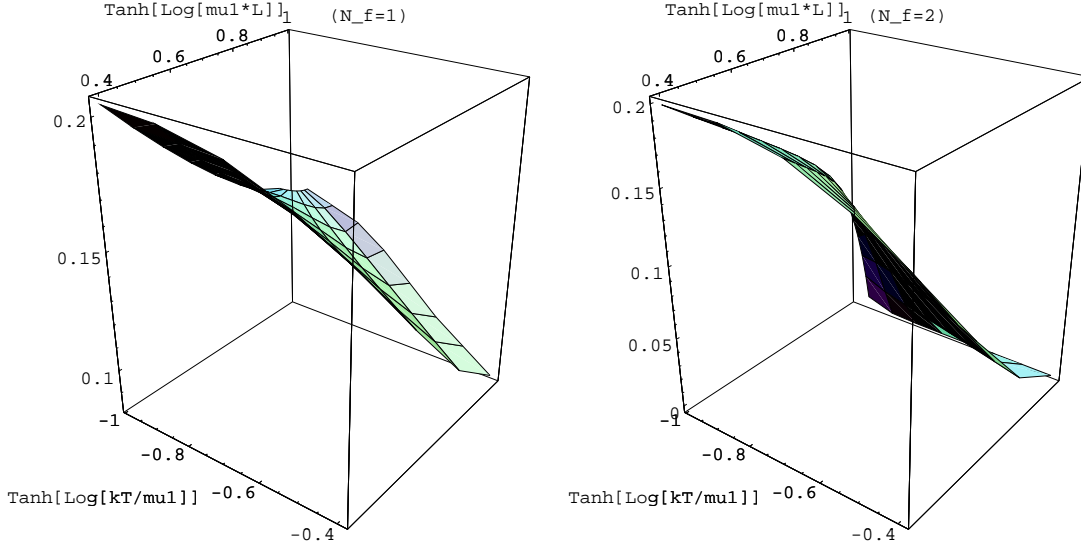


Figure 8: Zoom-out of the area $\sigma \gg 1, \lambda \gg 1$ (upper left corner in 7) for $N_f=1$ and $N_f=2$.

in the appendix) which has been done to get from (72, 73) to (74, 75).

At this point a pitfall arises: If, for the two-flavour case, the “alternative quantity” $2^{7/4} \pi^{1/2} e^{-\gamma} \cdot \sqrt{\lambda} |\langle \psi^\dagger P_\pm \psi \rangle| / \mu_1$ would be an order-parameter (actually it is *not* an order-parameter, as we shall see in a moment), the very fact that it acquires a finite value (1 in our normalization) at $\beta = L = \infty$ if the zero-temperature-limit is taken prior to the limit of infinite box-length while staying zero if the two limits are performed in reverse order would lead us to the (false) conclusion that at $\beta = L = \infty$ the system consists of two coexisting phases with relative weights which could be set by the way the point $\beta = L = \infty$ is approached: Following the corresponding “line of constant altitude” in the r.h.s. of figure 9 the relative weight of either phase (seemingly) could be given an arbitrary value between 0 and 1. This means that we would reach the (incorrect) conclusion that the two-flavour Schwinger model shows a first-order phase-transition with critical temperature $T_c=0$.

While the statement that the two-flavour Schwinger model exhibits a phase-transition at $T_c=0$ is indeed correct (see below), a classification as of first order is not – the transition is actually *second order*. To this end we shall first point out the fallacy in the above pseudo-reasoning and then present the correct argument.

The first question is: what is wrong in the argument which was declared to be a pitfall? The answer is: nothing is wrong – except for the fact that the if-condition is not fulfilled. The point is: the “alternative quantity” (the condensate times a factor $\sqrt{\lambda}$) is *not* an order-parameter. This might come as a surprise: Usually, in order to study critical phenomena or spontaneous symmetry breaking in field theory, the prescription is that one should choose an operator which is non-invariant under the symmetry in question. Then, in the presence of an external symmetry-breaking field, the vacuum-expectation-value of this operator for different temperatures and different external fields indicates the type of the phase-transition. In the case at hand the true order-parameter (the chiral condensate) and the “alternative quantity” differ from each other by a scalar factor, i.e. these two operators transform in the same way under a chiral transformation. Nevertheless, the correct order-parameter and the “alternative quantity” do not prove equally useful to study the chiral structure of the

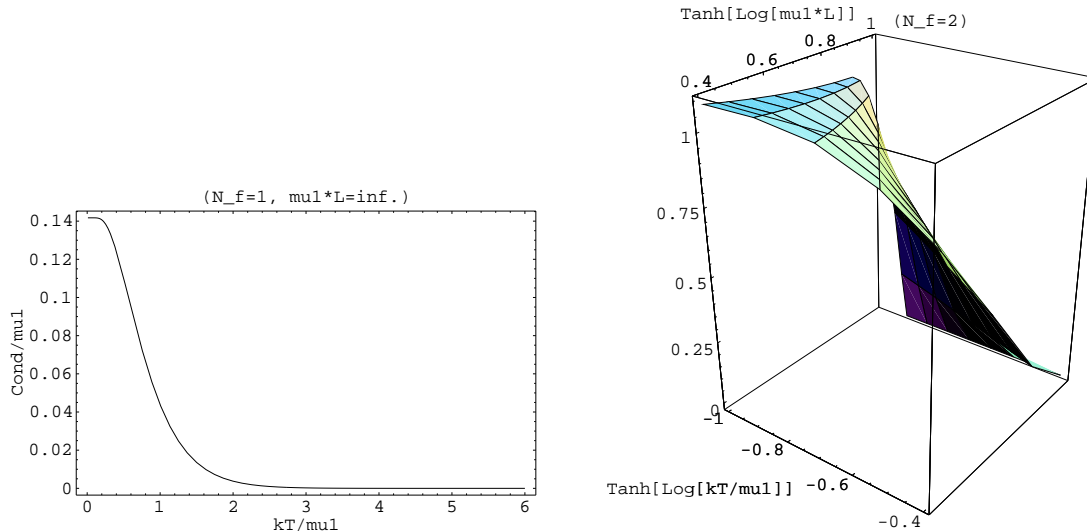


Figure 9: Left: The order-parameter $|\langle\psi^\dagger P_\pm\psi\rangle|/\mu_1$ of the one-flavour system as a function of the dimensionless temperature at infinite box-length. Right: Zoom-out of the upper left corner in the r.h.s. of figure 7 for the two-flavour system where the alternative quantity (*not an order-parameter !*) $2^{7/4}\pi^{1/2}e^{-\gamma} \cdot \lambda^{1/2}|\langle\psi^\dagger P_\pm\psi\rangle|/\mu_1$ is plotted rather than $\langle\psi^\dagger P_\pm\psi\rangle/\mu_1$ – providing direct numerical evidence for the noncommutativity phenomenon (77, 78).

theory: The “alternative quantity” can be seen as a specific member of a one-dimensional class of operators where the parameter is just the exponent of the prefactor λ in front of the condensate. Operators for which this parameter is smaller than $1/2$ tend to zero under $\lambda \rightarrow \infty$ whereas operators for which this parameter is bigger than $1/2$ diverge under $\lambda \rightarrow \infty$ (at zero temperature). Demanding this parameter to equal $1/2$ produces the finite jump at critical temperature shown in figure 9 but there is no physical meaning in this behaviour whatsoever: The “alternative quantity” $\propto \lambda^{1/2} \cdot |\langle\psi^\dagger P_\pm\psi\rangle|/\mu_1$ can not be used as an order parameter since its very definition either requires analytical knowledge about the behaviour of the condensate (which is the true order parameter) for large values of λ at zero temperature or so-to-say “critical tuning” which is completely intolerable. Moreover, even if we had overlooked this, the (incorrect) conclusion that the phase-transition is first order would not even be self-consistent: Whenever a system exhibits a true first-order transition a sufficiently small perturbation by the symmetry-breaking external field still leaves the transition first-order. This, however, is definitely not true for the case at hand: The condensate (and henceforth any operator in the one-dimensional set introduced above) was found to show an arbitrarily smooth crossover (as a function of σ) for any nonzero value of $1/\lambda$ (which, in our setting, plays the role of a small quark-mass term).

Having convinced ourselves that the condensate $|\langle\psi^\dagger P_\pm\psi\rangle|/\mu_1$ is the unique legitimate order parameter it is straightforward to read off the order of the phase-transition of the two-flavour system directly from the r.h.s. of figure 8: At zero temperature the condensate follows a “square-root” behaviour down to its limiting value (sc. 0) under $1/\lambda \rightarrow 0+$ whereas for any finite temperature it decays exponentially and henceforth such that even its derivative tends to zero under $1/\lambda \rightarrow 0+$. Thus there is no finite jump and no phase-coexistence at $T_c = 0$, the susceptibility (which, in our setting, is associated with the derivative of the condensate w.r.t.

$1/\lambda$) diverges under $1/\lambda \rightarrow 0+$ for $T=0$ like $1/\sqrt{(1/\lambda)}$ but tends to zero under $1/\lambda \rightarrow 0+$ for $T>0$ and the transition is *second order*.

4.8 Determination of δ

A system with a second order phase-transition exhibits a critical behaviour at its vicinity which is described by a set of critical exponents. While some of them refer to the broken phase and thus can not be defined in the case at hand, some other describe how the system behaves at or slightly above the transition under the influence of a symmetry-breaking external field and may be defined even if $T_c=0$.

In order to rephrase our results in the language of the usual approach where the infrared regulating and explicit chiral symmetry breaking device is the small fermion mass m rather than the inverse box-length $1/L$ one has to agree on how one of these two quantities shall be translated into the other one. It is clear that $1/L$ must be associated with a monotonic function of m . Sticking to the “naive” (i.e. dimensionally motivated) choice of identifying $1/L \leftrightarrow m$, the order-parameter in the massive zero-temperature Schwinger model is easily derived from (89) (for $N_f \geq 2$)

$$\lim_{T \downarrow 0} \langle \psi^\dagger P_\pm \psi \rangle \propto N_f^{1/2 N_f} m^{(N_f-1)/N_f} \exp \left\{ \frac{1}{N_f} \left(\gamma - 2 \sum_{j \geq 1} (-1)^j K_0 \left(j \sqrt{N_f} \frac{|e|}{m} \right) \right) \right\} \quad (81)$$

whereas at finite temperature the order parameter and its first derivative w.r.t. m still go to zero under $m \rightarrow 0+$. From this we learn two things:

(1) The phenomenon of a second-order phase-transition with zero critical temperature is not specific for the two-flavour model – the (massless) Schwinger model has a phase-transition at $T_c=0$ for *any number of flavours bigger than one*.

(2) The critical exponent δ which is defined through $\langle \psi^\dagger P_\pm \psi \rangle \propto m^{1/\delta}$ (at $T = T_c$) is $N_f/(N_f-1)$, i.e. $\delta=2$ for $N_f=2$ (upon identifying $1/L \leftrightarrow m$ – for a critical remark see below).

5 Discussion and Conclusion

The present paper has been devoted to a study of the N_f -flavour euclidean Schwinger model on a finite-temperature cylinder with $SU(N_f)_A$ breaking local boundary conditions at the two spatial ends. We have investigated the value of the dimensionless condensate $\langle \psi^\dagger P_\pm \psi \rangle / \mu_1$ at midpoints – which we used as order-parameter – as a function of the dimensionless inverse temperature $\sigma = \mu_1 \beta$ and box-length $\lambda = \mu_1 L$.

Our aim was to give a qualitative picture of the behaviour of the Schwinger model when quantized as described above. We found that on a logarithmic temperature-scale (with L kept finite but fixed) the condensate undergoes a well-localized crossover from a fairly constant value (at low temperatures) to a value which is exponentially close to zero at sufficiently high temperature – both for $N_f=1$ and $N_f=2$. From this we concluded that it is most reasonable to distinguish a (quasi-)phase with manifestly broken chiral symmetry from a quasi-phase where the chiral symmetry is almost restored – the distinction being done through a critical value of the condensate which was defined as half of the classical value of the condensate in the single-flavour model at zero temperature.

The numerical illustrations of our analytical results show that there is a qualitative difference in the behaviour of the single-flavour model as compared to the two-flavour model if

the combined limit of large box-length and small temperature is considered. For $N_f = 1$ the condensate takes a nonzero (T -dependent) value after $L \rightarrow \infty$. For $N_f = 2$ the condensate ends up being exactly zero under $L \rightarrow \infty$, but the way it approaches this limiting value is rather different for fixed $T = 0$ versus fixed $T > 0$: extremely reluctantly (i.e. $\propto 1/\sqrt{L}$) in the first case versus exponentially fast in the second case. This means that the susceptibility (defined as the first derivative of the condensate w.r.t. $1/L$) diverges in the two-flavour model like \sqrt{L} under $L \rightarrow \infty$ at zero temperature but tends to zero under $L \rightarrow \infty$ at any fixed finite temperature. This means that the two-flavour system exhibits a second-order phase-transition with critical temperature $T_c = 0$ – a result which was shown to extend to the cases $N_f \geq 3$. For $N_f = 1$, on the other hand, the order-parameter stays nonzero after $L \rightarrow \infty$ for any T , and the fact that it is just exponentially close but not equal to zero for $T \gg |e|$ illustrates the statement by Dolan and Jackiw that the one-flavour system never restores the anomalously broken $U(1)_A$ -symmetry at finite temperature [8].

It is worth emphasizing that the results summarized so far provide direct pictorial evidence for the claim by Smilga and Verbaarschot [9] which was based on an interesting indirect argument: These two authors used the result for the scalar susceptibility in the Schwinger model with degenerate massive flavours determined via bosonization rules and completed the list of critical exponents at small but nonzero temperature. Their result was that this list can be understood most easily as to consist of entries which satisfy the scaling relations for a system slightly above a second-order phase-transition with $T_c = 0$.

There is, however, one important point of numerical disagreement: Based on our analytical result plus the identification rule $m \leftrightarrow 1/L$ we have found the critical exponent $\delta = 2$ for the two-flavour system – which is at variance with the bosonization-rule based result $\delta = 3$ (which also agrees with the mean-field value) found in the literature [9].

As far as our part is concerned all we can say is that we have tried most diligently to make sure that our result is not due to an error in the analytical computations: Our finding for the numerical value of δ in the two-flavour case stems from (74) which was derived from (72). Through an explicit plot (figure 9) we tried to convince ourselves numerically that all the subleading factors in (72) do indeed get marginal in the zero-temperature limit and the overall λ -dependence tends to $1/\sqrt{\lambda}$ (for $N_f = 2$). Moreover numerical evaluations of (72) and (73) (after having cut down the infinite sums to an appropriate finite number of terms) were found to agree to more than a dozen decimal places for a large variety of σ - and λ -values.

As far as the result for δ in the literature is concerned all we can say is that the results for the massive Schwinger model we are aware of are based either on perturbation-theory in the fermion-mass [24] or on bosonization-rules (see [25] and references therein). While the original derivation of some of these rules was again within the mass-perturbation approach [26], the rules themselves seem not to be tied to perturbation-theory: Hetrick, Hosotani and Iso found in the bosonized massive Schwinger model with 2 or 3 degenerate flavours a noncommutativity-phenomenon between $m \rightarrow 0$ and $L \rightarrow \infty$ (where L plays in their scheme the role of a finite inverse temperature β) [27], which would be rather surprising if the bosonization-rules would not go beyond mass-perturbation theory. Nevertheless, for the bosonization rules to be applicable the condition $m \ll |e|$ has to hold true, whereas our results stem from an approximation-free analytical computation and are supposed to be exact for any inverse box-length and temperature.

At this point it should be stressed that the identification $1/\lambda \leftrightarrow m$ (which was necessary in order to extract, from our results, a value for δ in the usual approach where the symmetry breaking field is the quark-mass rather than the inverse box-length) is not canonical; a finite-

volume effect might, in principle, spoil the validity of our simple dimensionally motivated identification rule. Though this possibility seems rather unlikely, we feel that in the light of the known peculiarities of the two-dimensional world (the classical one being described in [7]) it can't be ruled out a priori. Needless to say that in the present situation both further analytical results in the massive multi-flavour Schwinger model and a determination of its critical indices from the lattice would be highly desirable. However, the fact that the critical temperature is zero provides a sort of a challenge for the lattice approach as it requires sophisticated reweighting techniques.

In summary we have presented a study of the chiral condensate in the one- and two-flavour finite-temperature Schwinger model in a quantization scheme where the usual quark-mass term is replaced by bag-inspired chiral symmetry breaking boundary conditions. Unlike results won from bosonization-rules or within mass-perturbation our formulas represent (hopefully) exact analytical findings gained through a straightforward evaluation of the path-integral. We have introduced the concept of *quasi-phases* in order to distinguish regions in the parameter-space where the symmetry under investigation is *manifestly broken* from those where it is *almost restored* and we have provided a direct pictorial verification of the claim by Smilga and Verbaarschot that the two-flavour Schwinger model undergoes a phase-transition at $T_c = 0$ and that the transition is of second order [9]. At the time being we are unable to resolve the discrepancy between our value for the critical exponent $\delta = N_f/(N_f - 1)$ and the bosonization-rule based result $\delta = (N_f + 1)/(N_f - 1)$.

Acknowledgments

It is a pleasure to acknowledge the hospitality received at the Institute for theoretical Physics of the University of Zürich where parts of this work were done. In addition, I would like to thank A. Wipf for a previous collaboration from which our investigation has taken benefit and an anonymous referee for pointing out an error in an earlier version of the manuscript. This work has been supported by the Swiss National Science Foundation (SNF).

Appendix

Here we shall give the details for the derivation of formulas (67, 68, 72, 73).

As one concentrates on the midpoints ($\xi = 1/2$), the r.h.s. of (63) takes the form

$$\begin{aligned}
(63) &= \pm \frac{e^{\pm\theta/\text{ch}(\lambda/2)}}{4\lambda} \sum_{n \in \mathbb{Z}} (-1)^n \frac{1}{\text{ch}(n\pi\tau)} \exp(-n^2\pi\tau) \cdot \\
&\quad \exp \left\{ 2 \sum_{n \geq 0} \frac{\text{cth}((2n+1)\pi\tau)}{(2n+1)} - ((2n+1) \rightarrow \sqrt{(2n+1)^2 + (\lambda/\pi)^2}) \right\} \\
&= \pm \frac{e^{\pm\theta/\text{ch}(\lambda/2)}}{4\lambda} \left(1 + 2 \sum_{n \geq 1} (-1)^n \frac{1}{\text{ch}(n\pi\tau)} \exp(-n^2\pi\tau) \right) \cdot \\
&\quad \exp \left\{ 2 \sum_{n \geq 0} \frac{1}{(2n+1)} - \frac{1}{\sqrt{(2n+1)^2 + (\lambda/\pi)^2}} \right\} \\
&\quad \exp \left\{ 4 \sum_{n \geq 0} \sum_{m \geq 1} \frac{e^{-2m(2n+1)\pi\tau}}{(2n+1)} - ((2n+1) \rightarrow \sqrt{(2n+1)^2 + (\lambda/\pi)^2}) \right\}
\end{aligned}$$

$$\begin{aligned}
&= \pm \frac{e^{\pm\theta/\text{ch}(\lambda/2)}}{4\lambda} \left(1 + 2 \sum_{n \geq 1} (-1)^n \frac{1}{\text{ch}(n\pi\tau)} \exp(-n^2\pi\tau) \right) \cdot \\
&\quad \exp \left\{ 2 \left(\frac{\gamma}{2} + \frac{1}{2} \log\left(\frac{\lambda}{\pi}\right) - \sum_{j \geq 1} (-1)^j K_0(j\lambda) \right) \right\} \\
&\quad \exp \left\{ 4 \sum_{n \geq 0} \frac{1}{(2n+1)(e^{2(2n+1)\pi\tau} - 1)} - ((2n+1) \rightarrow \sqrt{(2n+1)^2 + (\lambda/\pi)^2}) \right\} \quad (82)
\end{aligned}$$

which is the result (67) quoted in subsection 4.5 and where we used [22]

$$\sum_{j \geq 0} \frac{1}{2j+1} - \frac{1}{\sqrt{(2j+1)^2 + (x/\pi)^2}} = \frac{\gamma}{2} + \frac{1}{2} \log\left(\frac{x}{\pi}\right) - \sum_{j \geq 1} (-1)^j K_0(jx) \quad (83)$$

with $\gamma = 0.57\dots$ the Euler gamma and K_0 the modified Bessel function.

As one concentrates on the midpoints ($\xi = 1/2$), the r.h.s. of (64) takes the form

$$\begin{aligned}
(64) &= \pm \frac{e^{\pm\theta/\text{ch}(\lambda/2)}}{2\sigma} \sum_{m \in \mathbb{Z}} (-1)^m \frac{1}{\text{sh}(\pi(2m+1)/2\tau)} \times \\
&\quad \frac{\sum_{k \in \mathbb{Z}} e^{\pi(m+1/2)(2k+m+1/2)/\tau} (\text{erf}(\frac{(k+m+1)\sqrt{\pi}}{\sqrt{\tau}}) - \text{erf}(\frac{(k+m)\sqrt{\pi}}{\sqrt{\tau}}))}{2} \cdot \\
&\quad \exp \left\{ \pi \left(\frac{1}{4\tau} - \frac{\text{th}(\lambda/2)}{\sigma} \right) + \sum_{m \geq 1} \frac{\text{th}(m\pi/2\tau)}{m} - (m \rightarrow \sqrt{m^2 + (\sigma/2\pi)^2}) \right\} \\
&= \pm \frac{e^{\pm\theta/\text{ch}(\lambda/2)}}{2\sigma} \sum_{m \in \mathbb{Z}} (-1)^m \frac{1}{\text{sh}(\pi(2m+1)/2\tau)} \times \\
&\quad \frac{\sum_{k \in \mathbb{Z}} e^{\pi(m+1/2)(2k+1-m-1/2)/\tau} (\text{erf}(\frac{(1+(2k+1))\sqrt{\pi}}{2\sqrt{\tau}}) + \text{erf}(\frac{(1-(2k+1))\sqrt{\pi}}{2\sqrt{\tau}}))}{2} \cdot \\
&\quad \exp \left\{ \pi \left(\frac{1}{4\tau} - \frac{\text{th}(\lambda/2)}{\sigma} \right) + \sum_{m \geq 1} \frac{1}{m} - \frac{1}{\sqrt{m^2 + (\sigma/2\pi)^2}} \right\} \cdot \\
&\quad \exp \left\{ 2 \sum_{m \geq 1} \sum_{n \geq 1} (-1)^n \frac{e^{-2n(m\pi/2\tau)}}{m} - (m \rightarrow \sqrt{m^2 + (\sigma/2\pi)^2}) \right\} \\
&= \pm \frac{e^{\pm\theta/\text{ch}(\lambda/2)}}{\sigma} \sum_{m \geq 0} (-1)^m \frac{e^{-\pi((2m+1)^2-1)/4\tau}}{\text{sh}(\pi(2m+1)/2\tau)} \times \\
&\quad \sum_{k \geq 0} \text{ch}\left(\frac{\pi(2m+1)(2k+1)}{2\tau}\right) (\text{erf}(\frac{((2k+1)+1)\sqrt{\pi}}{2\sqrt{\tau}}) - \text{erf}(\frac{((2k+1)-1)\sqrt{\pi}}{2\sqrt{\tau}})) \cdot \\
&\quad \exp \left\{ \gamma + \log\left(\frac{\sigma}{4\pi}\right) + \frac{\pi(1 - \text{th}(\lambda/2))}{\sigma} - 2 \sum_{j \geq 1} K_0(j\sigma) \right\} \cdot \\
&\quad \exp \left\{ -2 \sum_{m \geq 1} \frac{1}{m(e^{m\pi/\tau} + 1)} - (m \rightarrow \sqrt{m^2 + (\sigma/2\pi)^2}) \right\} \quad (84)
\end{aligned}$$

which is the result (68) quoted in subsection 4.5 and where we used [22]

$$\sum_{j \geq 1} \frac{1}{j} - \frac{1}{\sqrt{j^2 + (x/\pi)^2}} = \gamma + \frac{\pi}{2x} + \log\left(\frac{x}{2\pi}\right) - 2 \sum_{j \geq 1} K_0(2jx) \quad (85)$$

with $\gamma = 0.57\dots$ the Euler gamma and K_0 the modified Bessel function.

As one concentrates on the midpoints ($\xi = 1/2$), the r.h.s. of (65) takes the form

$$\begin{aligned} (65) &= \pm \frac{e^{\pm\theta/\text{ch}(\lambda/\sqrt{2})}}{4\lambda} \sum_{n \in \mathbb{Z}} (-1)^n \frac{1}{\text{ch}(n\pi\tau)} \cdot \frac{\sum_{k \in \mathbb{Z}} e^{-k^2\pi\tau - (n-k)^2\pi\tau}}{\sum_{k \in \mathbb{Z}} e^{-2k^2\pi\tau}} \cdot \\ &\quad \exp \left\{ \sum_{n \geq 0} \frac{\text{cth}((2n+1)\pi\tau)}{(2n+1)} - ((2n+1) \rightarrow \sqrt{(2n+1)^2 + 2(\lambda/\pi)^2}) \right\} \\ &= \pm \frac{e^{\pm\theta/\text{ch}(\lambda/\sqrt{2})}}{4\lambda} \sum_{n \in \mathbb{Z}} (-1)^n \frac{1}{\text{ch}(n\pi\tau)} \cdot \frac{e^{-n^2\pi\tau/2} \sum_{k \in \mathbb{Z}} \frac{e^{-(n/2-k)^2 2\pi\tau} + e^{-(n/2+k)^2 2\pi\tau}}{2}}{\sum_{k \in \mathbb{Z}} e^{-2k^2\pi\tau}} \cdot \\ &\quad \exp \left\{ \sum_{n \geq 0} \frac{1}{(2n+1)} - \frac{1}{\sqrt{(2n+1)^2 + 2(\lambda/\pi)^2}} \right\} \\ &\quad \exp \left\{ 2 \sum_{n \geq 0} \sum_{m \geq 1} \frac{e^{-2m(2n+1)\pi\tau}}{(2n+1)} - ((2n+1) \rightarrow \sqrt{(2n+1)^2 + 2(\lambda/\pi)^2}) \right\} \\ &= \pm \frac{e^{\pm\theta/\text{ch}(\lambda/\sqrt{2})}}{4\lambda} \left(1 + 2 \sum_{n \geq 1} (-1)^n \frac{e^{-n^2\pi\tau/2}}{\text{ch}(n\pi\tau)} \cdot \frac{e^{-n^2\pi\tau/2} + 2 \sum_{k \geq 1} \frac{e^{-(n/2-k)^2 2\pi\tau} + e^{-(n/2+k)^2 2\pi\tau}}{2}}{1 + 2 \sum_{k \geq 1} e^{-2k^2\pi\tau}} \right) \cdot \\ &\quad \exp \left\{ \frac{\gamma}{2} + \frac{1}{2} \log\left(\frac{\sqrt{2}\lambda}{\pi}\right) - \sum_{j \geq 1} (-1)^j K_0(j\sqrt{2}\lambda) \right\} \\ &\quad \exp \left\{ 2 \sum_{n \geq 0} \frac{1}{(2n+1)(e^{2(2n+1)\pi\tau} - 1)} - ((2n+1) \rightarrow \sqrt{(2n+1)^2 + 2(\lambda/\pi)^2}) \right\} \quad (86) \end{aligned}$$

which is the result (72) quoted in subsection 4.5. and where we used (83).

As one concentrates on the midpoints ($\xi = 1/2$), the r.h.s. of (66) takes the form

$$\begin{aligned} (66) &= \pm \frac{e^{\pm\theta/\text{ch}(\lambda/\sqrt{2})}}{2\sigma} \sum_{m \in \mathbb{Z}} (-1)^m \frac{1}{\text{sh}(\pi(2m+1)/2\tau)} \times \\ &\quad \frac{\sum_{p \in \mathbb{Z}} \sum_{q \in \mathbb{Z}} \frac{1+(-1)^{p+q}}{2} e^{\pi((p+m+1/2)^2 - p^2 - q^2)/2\tau} (\text{erf}(\frac{p+m+3/2}{\sqrt{2\tau/\pi}}) - \text{erf}(\frac{p+m-1/2}{\sqrt{2\tau/\pi}}))}{2 \sum_{q \in \mathbb{Z}} e^{-\pi q^2/2\tau}} \cdot \\ &\quad \exp \left\{ \frac{\pi}{2} \left(\frac{1}{4\tau} - \frac{\text{th}(\lambda/\sqrt{2})}{\sqrt{2}\sigma} \right) + \frac{1}{2} \sum_{m \geq 1} \frac{\text{th}(m\pi/2\tau)}{m} - (m \rightarrow \sqrt{m^2 + 2(\sigma/2\pi)^2}) \right\} \\ &= \pm \frac{e^{\pm\theta/\text{ch}(\lambda/\sqrt{2})}}{2\sigma} \sum_{m \in \mathbb{Z}} (-1)^m \frac{e^{-\pi(m+1/2)^2/2\tau}}{\text{sh}(\pi(2m+1)/2\tau)} \times \end{aligned}$$

$$\begin{aligned}
& \frac{\sum_{q \in Z} e^{-\pi q^2/2\tau} \sum_{p \in Z} \frac{1+(-1)^{p+q-m}}{2} e^{\pi(p+1/2)(m+1/2)/\tau} (\operatorname{erf}(\frac{1+(p+1/2)}{\sqrt{2\tau/\pi}}) + \operatorname{erf}(\frac{1-(p+1/2)}{\sqrt{2\tau/\pi}}))}{2 \sum_{q \in Z} e^{-\pi q^2/2\tau}} \\
& \exp \left\{ \frac{\pi}{2} \left(\frac{1}{4\tau} - \frac{\operatorname{th}(\lambda/\sqrt{2})}{\sqrt{2}\sigma} \right) + \frac{1}{2} \sum_{m \geq 1} \frac{1}{m} - \frac{1}{\sqrt{m^2 + 2(\sigma/2\pi)^2}} \right\} \\
& \exp \left\{ \sum_{m \geq 1} \sum_{n \geq 1} (-1)^n \frac{e^{-2n(m\pi/2\tau)}}{m} - (m \rightarrow \sqrt{m^2 + 2(\sigma/2\pi)^2}) \right\} \\
& = \pm \frac{e^{\pm\theta/\operatorname{ch}(\lambda/\sqrt{2})}}{2\sigma} \sum_{m \in Z} (-1)^m \frac{e^{-\pi((2m+1)^2-1)/8\tau}}{\operatorname{sh}(\pi(2m+1)/2\tau)} \times \\
& \quad \frac{\sum_{q \in Z} e^{-\pi q^2/2\tau} \sum_{p \geq 0} \operatorname{ch}(\frac{\pi(p+1/2)(m+1/2)}{\tau}) (\operatorname{erf}(\frac{(p+1/2)+1}{\sqrt{2\tau/\pi}}) - \operatorname{erf}(\frac{(p+1/2)-1}{\sqrt{2\tau/\pi}})) +}{\sum_{q \in Z} e^{-\pi q^2/2\tau} \sum_{p \geq 0} (-1)^{p+q-m} \operatorname{sh}(\frac{\pi(p+1/2)(m+1/2)}{\tau}) (\operatorname{erf}(\frac{(p+1/2)+1}{\sqrt{2\tau/\pi}}) - \operatorname{erf}(\frac{(p+1/2)-1}{\sqrt{2\tau/\pi}}))} \\
& \quad \frac{2 \sum_{q \in Z} e^{-\pi q^2/2\tau}}{2 \sum_{q \in Z} e^{-\pi q^2/2\tau}} \\
& \exp \left\{ -\frac{\pi \operatorname{th}(\lambda/\sqrt{2})}{2\sqrt{2}\sigma} + \frac{1}{2} \left(\gamma + \frac{\pi}{\sqrt{2}\sigma} + \log\left(\frac{\sqrt{2}\sigma}{4\pi}\right) - 2 \sum_{j \geq 1} K_0(j\sqrt{2}\sigma) \right) \right\} \\
& \exp \left\{ -\sum_{m \geq 1} \frac{1}{m(e^{\pi m/\tau} + 1)} - (m \rightarrow \sqrt{m^2 + 2(\sigma/2\pi)^2}) \right\} \tag{87}
\end{aligned}$$

which is the result (73) quoted in subsection 4.5. and where we used (85).

For later use we finally mention that

$$\begin{aligned}
& \sum_{m \geq 0} (-1)^m \frac{e^{-\pi((2m+1)^2-1)/8\tau}}{\operatorname{sh}(\pi(2m+1)/2\tau)} \times \\
& \quad \frac{\sum_{q \in Z} e^{-\pi q^2/2\tau} \sum_{p \geq 0} \operatorname{ch}(\frac{\pi(p+1/2)(m+1/2)}{\tau}) (\operatorname{erf}(\frac{(p+1/2)+1}{\sqrt{2\tau/\pi}}) - \operatorname{erf}(\frac{(p+1/2)-1}{\sqrt{2\tau/\pi}})) +}{\sum_{q \in Z} e^{-\pi q^2/2\tau} \sum_{p \geq 0} (-1)^{p+q-m} \operatorname{sh}(\frac{\pi(p+1/2)(m+1/2)}{\tau}) (\operatorname{erf}(\frac{(p+1/2)+1}{\sqrt{2\tau/\pi}}) - \operatorname{erf}(\frac{(p+1/2)-1}{\sqrt{2\tau/\pi}}))} \\
& \quad \frac{\sum_{q \in Z} e^{-\pi q^2/2\tau}}{\sum_{q \in Z} e^{-\pi q^2/2\tau}} \\
& \simeq 4 * \exp\left(-\frac{\pi}{4\tau}\right) \tag{88}
\end{aligned}$$

for $\tau \ll 1$ and that the limit $\tau \rightarrow \infty$ for arbitrary N_f takes the form

$$\frac{\langle \psi^\dagger P_\pm \psi \rangle}{(|e|/\sqrt{\pi})} = \frac{e^{\pm\theta/\operatorname{ch}(\sqrt{N_f}\lambda/2)}}{4\lambda} \exp \left\{ \frac{\gamma}{N_f} + \frac{1}{N_f} \log\left(\frac{\sqrt{N_f}\lambda}{\pi}\right) - \frac{2}{N_f} \sum_{j \geq 1} (-1)^j K_0(j\sqrt{N_f}\lambda) \right\} \tag{89}$$

References

- [1] E.V.Shuryak: The QCD Vacuum, Hadrons and the Superdense Matter, World Scientific, Singapore (1988).
- [2] A.V.Smilga (Ed.): Continuous Advances in QCD, World Scientific, Singapore (1994).

- [3] J.Schwinger, Phys.Rev. **128**, 2425 (1962).
- [4] M.P.Fry, Phys.Rev. **D47**, 2629 (1993). C.Adam, Phys.Lett. **B363**, 79 (1995).
- [5] D.I.Diakonov, V.Petrov, Phys.Lett. **147B**, 351 (1984) and Nucl.Phys. **B245**, 259 (1984). E.Shuryak, J.Verbaarschot, Nucl.Phys. **B341**, 1 (1990) and **B410**, 55 (1993). T.Schäfer, E.Shuryak, J.Verbaarschot, Nucl. Phys. **B412**, 143 (1994). T.Schäfer, E.Shuryak, Phys.Rev. **D54**, 1099 (1996).
- [6] A.V.Smilga, Phys.Rev. **D46**, 5598 (1992). A.V.Smilga, Phys.Rev. **D49**, 5480 (1994).
- [7] S.Coleman, Comm.Math.Phys. **31**, 259 (1973).
- [8] L.Dolan, R.Jackiw, Phys.Rev. **D9**, 3320 (1974).
- [9] A.V.Smilga, J.J.M.Verbaarschot, Phys.Rev. **D54**,1087 (1996).
- [10] J.H.Loewenstein, J.A.Swieca, Ann.Phys. **68**, 172 (1961). N.K.Nielsen, B.Schroer, Nucl.Phys. **B120**, 62 (1977). K.D.Rothe, B.Schroer, Phys.Rev. **D20**, 3203 (1979). N.V. Krashnikov et al, Phys.Lett. **B97**, 103 (1980). R.Roskies, F.Shaposnik, Phys.Rev. **D23**, 558 (1981). A.K.Raina, G.Wanders, Ann.Phys. **132**, 404 (1981). A.Z.Capri, R. Ferrari, Nuov.Cim. **A62**, 273 (1981). P.Becher, Ann.Phys. **146**, 223 (1983).
- [11] C.Gattringer, E.Seiler, Ann.Phys. **233**, 97 (1994).
- [12] C.Jayewardena, Helv.Phys.Acta **61**, 636 (1988).
- [13] I.Sachs, A.Wipf, Helv.Phys.Acta **65**, 652 (1992).
- [14] T.Banks, A.Casher, Nucl.Phys. **B169**, 103 (1980).
- [15] A.Wipf, S.Dürr, Nucl.Phys. **B443**, 201 (1995).
- [16] P.Hrasko, J.Balog, Nucl.Phys. **B245**, 118 (1984).
- [17] S.Dürr, A.Wipf, Ann.Phys. **255**, 333 (1997).
- [18] H.A.Falomir, R.E.Gamboa Saravi, M.A.Muschietti, E.V.Santangelo, J.E.Solomin, hep-th/9608101 and hep-th/9608102.
- [19] E.Merzbacher, Quantum Mechanics, Wiley, New York (1961).
- [20] J.S.Dowker, R.Critchley, Phys.Rev. **D13**, 3224. (1976). S.W.Hawking, Commun.Math. Phys. **55**, 133 (1977).
- [21] E.Elizalde, S.G.Odintsov, A.Romeo, A.A.Bytsenko, S.Zerbini: Zeta Regularization Techniques with Applications, World Scientific, Singapore (1994).
- [22] I.S.GradshTEyn, I.M.Ryzhik: Table of Integrals, Series and Products, Fifth Edition, Academic Press, San Diego (1995).
- [23] M.Abramowitz, I.A.Stegun: Handbook of Mathematical Functions, Dover Publications, New York (1970).
- [24] C.Adam, Ann.Phys. **259**, 1 (1997).
- [25] S.Coleman, Ann.Phys. **101**, 239 (1976). A.V.Smilga, Phys.Lett. **B278**, 371 (1992). Y.Hosotani, R.Rodriguez, hep-th/9804205.
- [26] S.Coleman, Phys.Rev. **D11**, 2088 (1975).
- [27] J.E.Hetrick, Y.Hosotani, S.Iso, Phys.Lett. **B350**, 92 (1995). J.E.Hetrick, Y.Hosotani, S.Iso, Phys.Rev. **D53**, 7255 (1996).